DLR-IB-RM-OP-2020-22

Development of a Tactile Thimble for Augmented and Virtual Reality Applications

Masterarbeit

Suraj Giri

DLR Deutsches Zentrum für Luft- und Raumfahrt

Institut für Robotik und Mechatronik	BJ.: 2020
	IB.Nr.: DLR-IB-RM-OP-2020-22

MASTERARBEIT

DEVELOPMENT OF A TACTILE THIMBLE FOR AUGMENTED AND VIRTUAL REALITY APPLICATIONS

Freigabe:	Der Bearbeiter:	Unterschriften
	Suraj Giri	Suraj S Giri
	Betreuer:	
	Thomas Hulin	
	Der Institutsdirektor	
	Prof. Alin Albu-Schäffer	

Dieser Bericht enthält 84 Seiten, 33 Abbildungen und 7 Tabellen

Ort: Oberpfaffenhofen	Datum: 06.02.2020	Bearbeiter: Suraj Giri	Zeichen:

UNIVERSITÄT SIEGEN

DEPARTMENT MASCHINENBAU

Institut für Konstruktion

Lehrstuhl für Produktentwicklung

MASTER'S THESIS

Development of a Tactile Thimble for Augmented and Virtual Reality Applications

by

Suraj GIRI

Examiners (University of Siegen):
Prof. Dr.-Ing. Tamara REINICKE
M. Sc. Nithin PADAVU

Supervisors (German Aerospace Center):
Dr. Thomas HULIN
Dr. Harsimran SINGH

DLR

December 23, 2019

I, Suraj GIRI, declare that this thesis titled, "Development of a Tactile Thimble for Augmented and Virtual Reality Applications" is written independently and have used no sources or resources other than those specified.

Hiermit versichere ich, dass ich die vorliegende Arbeit selbständig verfasst und keine anderen als die angegebenen Quellen und Hilfsmittel benutzt habe.

Signed:

Place, Date: 23.12.2019, Siegen

Sperrvermerk

Die vorgelegte Masterarbeit basiert auf internen, vertraulichen Daten und Informationen das Deutsche Zentrum für Luft- und Raumfahrt (DLR). In diese Arbeit dürfen Dritte, mit Ausnahme der Gutachter und befugten Mitgliedern des Prüfungsausschusses, ohne ausdrückliche Zustimmung das DLR und des Verfassers keine Einsicht nehmen. Eine Vervielfältigung und Veröffentlichung der Masterarbeit ohne ausdrückliche Genehmigung – auch auszugsweise – ist nicht erlaubt

Abstract

Development of a Tactile Thimble for Augmented and Virtual Reality Applications

The technologies that have gained a renewed interest during the recent years are Virtual Reality (VR) and Augmented Reality (AR), as they become more accessible and affordable for mass-production. The input device which allows us to interact with the virtual environment is a very crucial aspect. One of the main barriers to immerse ourselves in virtual reality is the lack of realistic feedback. The user has to almost rely entirely on visual feedback without any haptic feedback, and this increases the user's workload and decreases the performance.

In this thesis, a functional demonstrator of a tactile feedback device which conveys compelling interactions with not just VR, but also AR is presented. The device is designed such that there is realistic feedback for virtual touches and least obstruction during contact of a real object in AR applications. New design principle of introducing small actuators allows the device to be compact and increases its portability.

In contrast to actuators that are placed on the finger pad in most of the available input devices for VR, a tactile device with two actuators that are arranged laterally on the finger, so that the underside of the fingertip is free is proposed. The output from these actuators generate a tactile stimulus by stimulating a sense of touch, which helps the user to manipulate virtual objects. The actuators are designed to independently generate vibrations and this coupled tactile feedback enhances the stimulation resulting in a wide variety of stimulation patterns for the sense of touch. Preliminary experimental evaluation for design and location of actuators has been carried out to measure the vibration intensity. In addition, user experiments for design evaluation of the two actuators based on different vibration patterns have also been conducted.

Contents

List of Figures

List of Tables

Acronyms

VE Virtual Environment

VR Virtual Reality

AR Augmented Reality

HCI Human - Computer Interface

GUI Graphical User Interface

SAW Surface Acoustiv Waves

ETS Electro Tactile Stimulation

ERM Eccentric Rotary Motors

LRA Linear Resonant Actuator

EAP Electroactive Polymer

DEA Dielectric Elastomer Actuator

CNT Carbon Nanotube

SMA Smart Memory Alloy

IoT Internet of Things

ToF Time of Flight

GPIO General Purpose Inout/Output

PWM Pulse-width Modulation

I2C Inter-integrated Circuit

FDM Fused Deposition Modeling

PP Polypropylene

PLA Polylactic acid

AE Augmented Environment

Chapter 1

Introduction

Haptics refers to 'sense of touch', which in every situation helps us understand the outside world and perform various tasks. It contains good penetrable capacity which can pass through intensive receptors present on our skin. This sense of touch can be artificially recreated by stimulating different parts of our body (commonly the hands) in robot teleoperation and virtual environments (VEs). It is achieved by recreating the important features of touch to increase realism and performance.

The sense of touch appears to be fundamental to assess the properties of a product. This has become more evident as visual and auditory feedback are not sufficient to completely recognise the objects. The impact from the combination of sensory input and haptics has definitely motivated different disciplines such as biomechanics, computer science, medical and aeronautics to analyze force feedback with VEs. This gives the human operators a sense of 'telepresence', so that they feel they are directly manipulating the objects and their environment. Absence of haptic feedback may lead to misinterpretation in the virtual world. For example, a user trying to interact with a virtual object with the aid of visual feedback can see the contact with the ball, but there is no barrier to stop the user from passing through the ball. It can therefore be said that while traditional sensing methods like laser, audio and vision sensors are fast approaching a level of saturation, further advancements should rely on other sensing modalities. Additional sensing modalities could enhance the performance and allow robust manipulation of objects in the field of teleoperation and VR. More inputs and feedback also save energy by reducing the margin of error and the time taken to complete the task.

1.1 Problem Definition and Approach

Haptic interfaces are mechanical devices that help the user to communicate with a computer system. It is in charge of reproducing what is captured in the sensation of contact or manipulation of an object, and allows the user to touch, feel and manipulate 3-Dimensional objects in VE. A number of haptic devices exist which allow users to communicate through the sense of touch. For interaction with 3D objects, the haptic feedback can be divided into two groups: kinesthetic feedback and tactile feedback. Kinesthetic feedback can reproduce the weight of the grasped virtual object as well as motion constraints. Whereas, tactile feedback such as temperature and vibrations is felt by the skin. It deals with the information that is distributed as tactile force over the region of contact, and simulate that contact to the skin.

The goal of this Thesis is to develop a device which generates tactile actuation on the fingertip. The device serves as a human-machine interface for virtual reality (VR) applications and for the person wearing the device, the sense of touch can be simulated on at least one of the fingers. This gives an impression of manipulating or touching a virtual object. To provide tactile feedback for VR, most researchers construct complex and heavy mechanical actuators for tactile stimulation on the user's fingers. This can have a negative effect on the user's experience as it makes them more aware of the cumbersome hardware on their physical body. The user is more conscious of the feedback device due to its bulkiness, which may diminish a truly immersive experience. Moreover, most of the vibration feedback devices use DC motors, which have limited amplitude and frequency bandwidth. As both the frequency and amplitude of vibration cannot be modulated independently, wide range of sensations cannot be achieved.

To overcome these drawbacks, a comparitive study of the different haptic technologies is undertaken. In most of the tactile devices, the finger pads (the surface opposite to the fingernail that has characteristic of a human fingerprint) are covered. In terms of construction, one of the important requirement is to improve the device in such a way that any contact with an object in the real world is obstructed as little

as possible while at the same time, having most realistic feedback during interactions in the VE. The device should be designed in such a way that the underside of the fingertip (which is also referred to as phalanx distal) is freely accessible and can touch objects. In other words, the underside of the finger tip first comes in contact with an object and the device does not interfere or obstruct when the user is touching an object, nor falsify the impression of touch. Furthermore, the device should consist of two output units and each of these output units consists of a controllable actuator which can generate force and/or moment that is transmitted to the finger tips. Some of the examples of different actuators are shape memory alloys, electroactive polymers, piezo elements, etc. Having two different output units helps to generate aperiodic forces and vibrations, so that the tactile stimulus can be varied locally and in intensity over the area of the fingertip. Advantageously, this results in further degrees of freedom for the stimulation of the sense of touch on the fingertips. In consequence, having a lightweight device without any obstruction on the finger pads makes the user comfortable to interact with virtual objects and real objects simultaneously, without having to remove the device.

1.2 Practical Outline

The work conducted during this Thesis comprises of literature study, electronic circuit development, mechanical design and testing of a tactile device with respect to the gathered requirements. The Thesis is organized as follows:

- **Chapter 2** - "Background" gives an overview on basic subjects that are relevant for this Thesis. Special terms related to haptics and human senses are explained here.
- **Chapter 3** - "Tactile Actuation Technologies" takes a closer look on different methods of tactile stimulation, mainly focusing on vibrotactile feedback.
- **Chapter 4** - "Design Guidelines and Hardware Setup" describes the design guidelines and the hardware components necessary to develop the proposed device.

- **Chapter 5** - "System Implementation" provides information on software development, in which the hardware components are interfaced to perform stand alone tests.
- **Chapter 6** - "Mechanical Design" describes the construction and fabrication of the tactile device, and explains the physical design considerations.
- **Chapter 7** - "Evaluation Study" takes a closer look on how the device works in realistic conditions, by conducting tests with different participants.
- **Chapter 8** - "Conclusion" sums up the results of all the previous chapters. It also provides interesting recommendations on future research in the field of wearable systems and tactile devices.

Chapter 2

Background

In this chapter, literature review relevant to current knowledge and achievements in the field of haptic systems is carried out. The theoretical background is described to better understand the development process within the thesis. In the first part, the basic functioning of haptic devices and their applications is discussed. Later, relevant literature on human somatosensory system or sense of touch is explored. Also, different tactile actuation technologies and the functionality of existing haptic displays is discussed.

2.1 Haptics

Haptic Human-Computer interaction is one of the forms of interaction between a computer and a human computer user based on sense of touch. With new technological developments, the research on interaction between computers and humans is more relevant in the recent years [BMS03]. In particular, the input devices for immersive interactions with objects in VEs, leading to advancements in haptic interaction and feedback.

2.1.1 Haptic Interface components

Unlike traditional feedback interfaces like auditory and visual information, haptic interfaces provide humans a way to change their environment, and stimulate kinesthetic and touch channels through mechanical signals. Therefore, Haptics is classified as one of the areas of Human-Computer Interface (HCI).

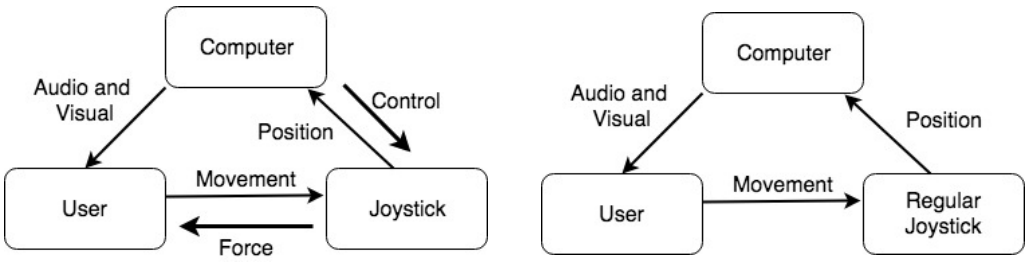

(A) Haptic interface (B) Traditional interface

FIGURE 2.1: Comparison of haptic and traditional interfaces.

To discuss the functioning of a haptic interface, just like in any other interface, we consider an input device and a display device. The basic difference between a haptic interface and a conventional (regular joystick) interface can be understood from Figure. 2.1. With the arrows representing the direction of information flow, it is observed that a regular joystick is limited to unidirectional input to the computer. The user almost receives no feedback information from its movements but however, with a haptic joystick, a programmable feedback based on the sense of touch helps with better intuitive interaction with the computer. The haptic system in combination with visual and audio systems usually contains two interfaces, a computer interface and a human interface. The haptic system receives the control information from the computer and sends position signals back to the computer interface. The interface helps the user to feel the VE by providing different kinds of perceptual information. This provides the user with an integrated perception in applications such as virtual manufacturing, medical training and entertainment.

2.1.2 Haptic Device Applications

The research and development of haptic devices for VEs is expanding and its application spans a wide range of fields, both research oriented and commercial. Some of the main application fields of these devices are briefly discussed below:

(a) Virtual Manufacturing In manufacturing, haptic systems can change the traditional design and manufacturing approaches mainly based on mock-ups and CAD, by benefiting from realistic force/torque feedback. It diminishes the gap between the real and virtual world as it helps with handling the objects intuitively

during the virtual assembly process. It is also possible to facilitate programming of complex manufacturing machines such as robots. [MPT05]

(b) Medical Training Medical procedures already involve the use of tactile sensing to a great extent and haptic devices, with a sense of touch during virtual simulation, can be used as a training alternative to provide sufficient experience. Haptic interfaces can especially be useful for minimal invasive procedure and remote surgery using teleoperators. One such device is MIMIC Technologies's (Seattle, USA) Da Vinci Trainer [MT19] which is already being used to train operators on robotic surgery.

(c) Entertainment Haptic devices are already being used commercially for simulation in games, pilot simulators, automobile driving, etc. The feedback from the haptic devices can be translated in improving the skills of players playing. Common game devices such as joysticks and game-pads are constantly being improved to enhance the immersive experience by applying force feedback to the game player.

Some of the other application scenarios for haptic devices [HACH+04] are:

- *GUIs feedback reinforcements*, like buttons and pull-down menus.
- *Data and science analysis*, for data-mining, geology, maps
- *Rehabilitation*, to improve and support the conditions of disable people
- *Arts and creation*, for visual communication channels
- *Education and training*, for example, Astronaut training and other innovative passive learning methods
- *Vehicle industry*, better interaction with the vehicle for more intuitive control.

2.2 Sense of Touch

The human sense of touch is the combination of two different classes of sensory information known as kinesthesia and tactile perception. The Figure 2.2 illustrates different senses in a human body.

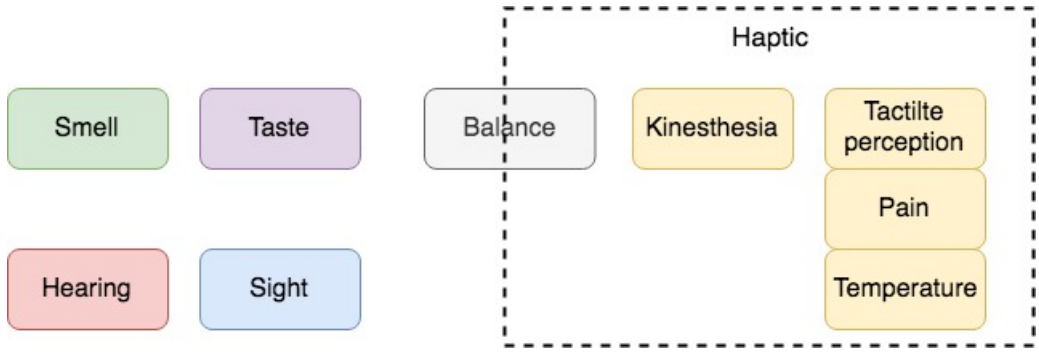

FIGURE 2.2: Human senses. Based on [Ker08]

2.2.1 Kinesthesia

Kinesthesia or kinesthetic feedback refers to the information perceived by the receptors in muscles, joints and tendons, and this information is reproduced as force feedback in a haptic interface [CSO18]. The information contains position, torque and weight of different body parts associated with muscles and tendons. This allows the user to recognize the weight, inertia and motion of the grasped object [Bur96].

2.2.2 Tactile Perception

In contrast to kinesthetic feedback, tactile perception refers to sensation arising from the skin due to contact. It is perceived through the nerve endings under the surface of the skin and allows to process various sensations such as pressure, vibration and temperature [JS08]. As this thesis deals with tactile stimulation, and kinesthetic sensory system is not involved, focus is mainly on mechanoreceptors in the skin. An understanding of different types of receptors on the surface of our skin and their properties will help facilitate the types of feedback devices discussed later.

Figure 2.3 shows the general structure of a hairy human skin. Each of the layers under the skin consists of different types of mechanoreceptors for different perceptions. There are four types of them: Meissner Corpuscle, Merkel disks, Pacinian corpuscle and Ruffini corpuscle. They are classified based on the size of receptive fields (small (I) and large(II)) and the nerve endings they are connected to (fast adapting (FA) and slow adapting (SA)) [GWV09, Ske12]. The receptors which have small receptive fields respond to high spacial acuity (the ability to resolve fine details).

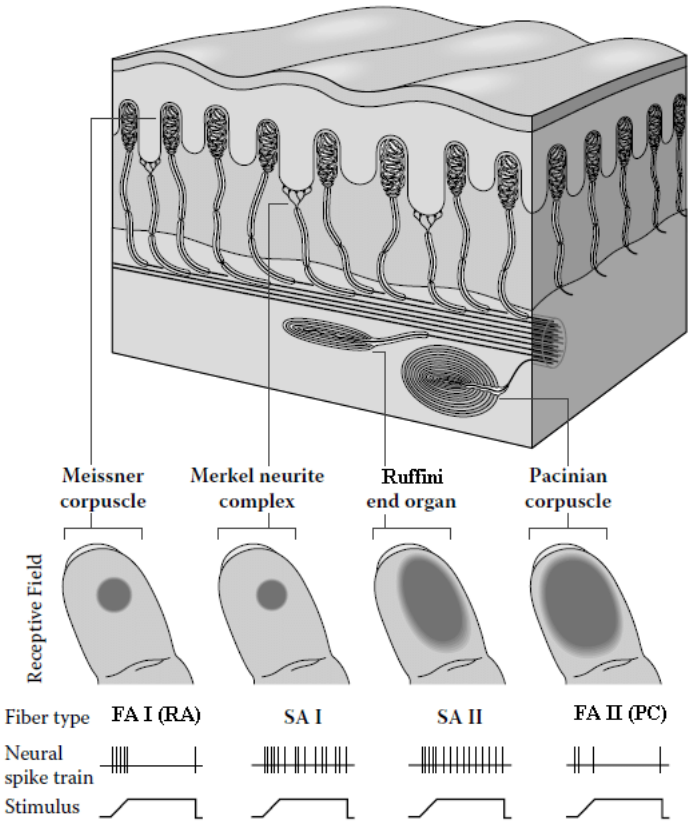

FIGURE 2.3: Mechanoreceptors in glabrous skin [GWV09]

As seen in the figure, the fast-adapting fibers produce neural spikes only at the beginning and at the end of stimulation. While the slow-adapting fibers produce the neural spikes during the entire stimulation period. Meissner and Pacinian corpuscle are rapidly adapting mechanoreceptors, which means they can quickly react to tactile stimuli. In contrast, Merkel's discs and Ruffini corpuscles are slow-adapting and they slowly react to the stimuli. Table 2.1 summarizes the classification of these mechanoreceptors and their properties. [Ver66]

Sensory substitution is the concept of communication information from external sources (partially to replace a new sense or create a new one). The nervous system can learn to interpret the information with subsequent training and the substitution device should be very intuitive with good information bandwidth. Similarly, a number of devices have been developed that stimulate these mechanoreceptors in one way or the other. Some of the most commonly used devices either use vibration or electrical stimulation. With the help of electrodes placed on the skin and by

TABLE 2.1: Functional Characteristics of Mechanoreceptors beneath the human skin. Adapted from [CK12, Ske12]

Characteristics	**Merkel Disks**	**Ruffini ending**	**Meissener Corpuscle**	**Pacinian Corpuscle**
Adaptation Rate	Slow (SA-I)	Slow (SA-II)	Fast (FA-I)	Fast (FA-II)
Spacial Resolution	Good	Fair	Poor	very Poor
Median Field Size (mm^2)	11	1.4	113	n/a
Frequency Range (Hz)	0.4 - 10	0.4 - 100	10 - 200	70 - 1000
Sensitivity	Pressure: deformation in spacial structure	Stretch: laterial deformation	Flutter: deformation changes, movement or light touch	Vibration: deformation changes, movement or fine textures

injecting electric current, the electrotactile stimulation devices can communicate by artificially stimulating the mechanoreceptors [IKB+03, KWByRT91]. These devices can stimulate responses such as pressure, pain, temperature and vibration, which can often be uncomfortable, as the current threshold required, depends on the diameter of the nerve fiber and depth under the skin. A detailed study is undertaken in the next section.

Additionally, tactile perception and tactile devices can also be classified based on two types of stimulation, namely active and passive touch.

- In active touch, the user is in control of his/her own actions. With the information such as surface texture and edges obtained from moving the finger over a surface, the brain can rapidly identify the object.[Gib66]

- In passive touch, the haptic device is controlled under motor control. An example is someone's hand pressed against an object, where a body part that is resting is in contact with the object. [SSCR01]

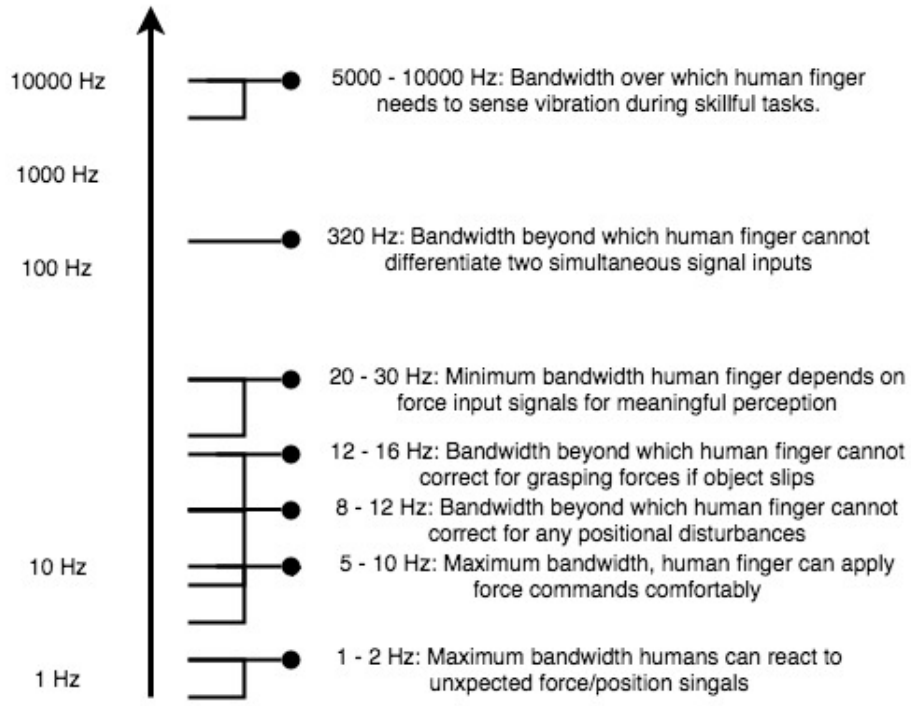

FIGURE 2.4: Sensitivity bandwidth of a human finger. [BB96]

2.3 Haptic Feedback Systems

This section situates the work within the space of existing haptic devices. As mentioned in the previous section, haptic devices are typically divided into: kinesthetic and tactile devices.

2.3.1 Kinesthetic devices

A large number of different types of haptic devices have been developed for various applications in the last decade. One such experimental system is the Augmented Mouse with two haptic features by Akamatsu *et al.* [ASM94]. One feature is the vibro-tactile sensations by using a transducer and the other is an electromagnetic braking system, which provides a linear, programmable physical damping. For haptic feedback in a graphical user interface, a two degrees of freedom trackball like device was developed.

Several VR Gloves have also been developed, such as the *CyberGrasp Glove*. The haptic glove, shown in Figure 2.5a, is a hand-worn exoskeleton that restricts finger motion when grasping a virtual object and thereby, integrating force feedback. The

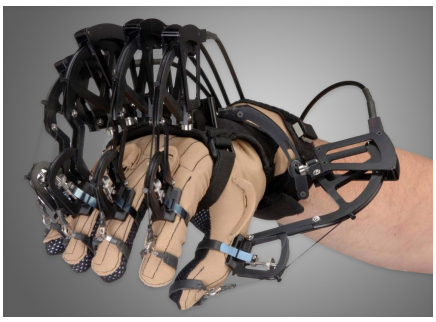

(A) The Cybergrasp Glove by CyberGlove Systems LLC. [Bur00]

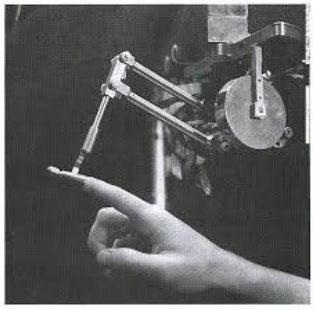

(B) The PHANToM Haptic Interface. [MS+94]

FIGURE 2.5: Force-Feedback Haptic Devices

workspace is about 12x12in. with a radius of 20in. swept through 133° [LLC19]. One of the most iconic devices is the *PHANTOM* with combination of both force and tactile feedback (See Figure 2.5b). *Phantom* allows users to feel virtual objects by applying a controlled force to the finger. Its workspace is equal to the size of a computer keyboard. [MS+94]

An application of surround haptics was presented by Israr *et al.* [IEVO09] that uses vibrotactile actuators embedded on a chair to generate continuous tactile strokes on the skin, for a driving simulation game. For different events such as collision, acceleration and tire traction, the actuators provide different sensation.

2.3.2 Cutaneous devices

The main approach that is required to implement and evaluate during this thesis, is the cutaneous or the tactile feedback approach for VEs. In this subsection, some of the existing haptic displays with tactile sensation is discussed. Tactile feedback such as vibration adds another information channel while interacting with Mobile Augmented Reality (MAR) environment, and benefits the user moving an icon, or touching it. Chinello *et al.* [CMPP15] presents a wearable tactile device (3-RRS fingertip device, see Figure 2.6a), that uses servo motors to move a rigid platform under the fingertip. The upper static body supports three small servo motors that drives the rigid platform to provide contact deformation stimulus on the user's fingertip. Pacchierotti *et al.* presents a 2-DOF haptic device which consists of a fabric belt along with two servo motors. As seen in Figure 2.6b, the fingertip is completely free as the

device is worn on the finger's proximal phalanx and this helps the user interact with hand-tracking devices like Leap Motion. The belt is driven by the two servo motors to provide sheer and normal stimuli to the user's finger. [PPK15]

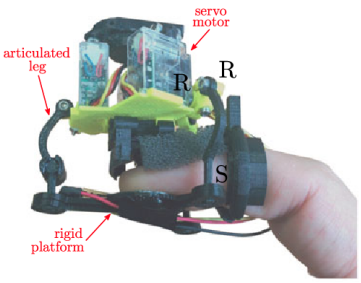

(A) 3-RRS Fingertip Device [CMPP15]

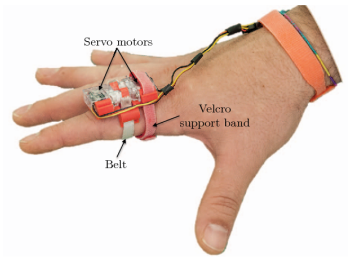

(B) The hRing: A wearable haptic device to avoid occlusions in hand tracking. [PSH+16]

FIGURE 2.6: Wearable Fingertip Haptic Devices

In [MPC+17], these two cutaneous devices (shown in Figure 2.6) are evaluated based on different AR tasks such as picking and moving a virtual object, and hand writing. The experiments use visual markers and cameras mounted on Oculus Rift HMD for hand-tracking, creating a AR scenario. Though the 3-RSS device outperforms the hRing in one of the experiments, the hRing device is preferred due to its construction as it leaves the fingertip free for real world interactions.

2.4 Chapter Summary

Though there have been a lot of progress in the integration of haptic feedback for VEs so far, further improvements are needed more importantly in terms of resolution, frequency bandwidth and compactness to account for higher realism. In this chapter, basic perceptive principles that are relevant for designing devices with vibrotactile patterns are presented. Also, some of the existing haptic devices, which resort to different actuators to recreate the touch sensations are introduced. In the next chapter, different actuator technologies and evaluate them, to help develop a lightweight, easy to use and cost effective prototype for virtual and augmented environments are discussed.

Chapter 3

Tactile Actuation Technologies

Ideally, the tactile displays should refresh in real time to keep up with the rapidly changing inputs. This also means that the device should be able to convey new information as quickly as the mechanoreceptors in the human skin can react. Compared to static patterns, humans are more sensitive to tactile stimuli that are moving or changing [DCMD00]. Therefore, the information coded by the display should also be a simulated motion against the fingertips. To also make the display more intuitive and easy to learn, the display should code the information can be easily interpreted. Lastly, to ensure that the costs are low, the device should be manufacturable by efficient means and its power consumption should be consistent for portable use. In this chapter, the different methods of tactile actuation technologies are explored, and their advantages and disadvantages are investigated.

3.1 Methods of Tactile Stimulation

The stimulation methods can approximately be divided into three categories: mechanical, thermal and electrical stimuli.

3.1.1 Mechanical

Mechanical stimulation is one of the most commonly used methods on tactile displays because when compared to electrical and thermal stimulation, this has finer

spatial resolution [XLY+17]. Also, the mechanoreceptors tend to respond to physical mechanical stimuli easily. The most common examples that belong to mechanical actuation principle are:

- Static indentation
- Vibration
- Surface acoustic waves
- Magnetorheological fluids

Static Indentation

The most common category of static indentation information is a braille device. Braille reader consists of different dots of braille cells that are driven up and down by an array of stacked piezoelectric bending beam actuators. It is an excellent means of providing text information for people who understand braille literacy. This can be achieved by scanning the information using an optical character recognition or if the information is electronically available as text [Fie98]. A refreshable braille display is an electro-mechanical device that displays characters by means of pins raised through holes on a flat surface. This provides an opportunity for visually impaired users who cannot use a monitor to read output.

Vibration

As discussed in Chapter 2, the fast adapting mechanoreceptors (Meissner and Pacinian corpuscles) on our skin are stimulated by rapidly changing stimulus and they can sense vibration better than static indentation [LN99]. Vibrotactile stimulation is the most widely method of stimulation in tactile displays due to its lower threshold of force and displacement of vibration, when compared to static indentation. As human beings, one can distinguish vibration pulses better than our vision system. Our vision system has a minimum time gap of $25ms$ as compared to the time gap of successive vibration pulses of $5ms$ [GWV10]. This means that different variations

of vibration patterns can be effectively realized by changing the amplitude and frequency of vibration to provide information with complex meaning.

Surface Acoustic Waves

The waves generated by SAW transducers can be used to provide an intuitive sensation of continuous roughness on the skin. In this case, active tactile transducers utilize standing waves and shift in friction to generate vibration. In contrast, ultrasonic motors are described as passive type transducers that generate vibration directly on the user's finger [TKMN04, NTM+01].

Magnetorheological Fluids

Magnetorheological fluids are materials that respond to magnetic field and have been used to make tactile devices. They consist of ferromagnetic particles (1-100μm) that are sensitive to the potential of magnetic field. They remain in liquid form when there is no magnetic stimulus and upon application of magnetic field, the particles align themselves parallel to the direction of the field. This causes a change in viscosity and the liquid becomes a solid gel as the field increase. [SFRS04]

3.1.2 Thermal

The combination of both vibrotactile and thermal stimulation is used in various devices for generating haptic sensation. A 3x3 device has been developed by [Mao14], to produce different distributions between 5°C and 55°C with the help of multiple heat sources. Thermal sensation models developed for a fingertip also shows that the skin is more sensitive to rapid change in temperature, which leads to difficulty in generating long duration's of stimulation [YCHH04]. Despite these advantages, thermal tactile displays are not well-suited to provide rich information because of their low transition-sensing time between on/off states and low spacial resolution [JSZM15].

3.1.3 Electrotactile

Electrotactile stimulation (ETS) uses electric current from the electrodes in the device to provide tactile sensation to the mechanoreceptors on the skin [ST70]. These actuators can mimic pressure and vibration without the need of mechanical actuators. SmartTouch is a 4x4 tactile matrix developed to selectively stimulate Meissners corpuscles and Merkel's discs. The electrodes in these devices run electric pulses of 1-3 mA with a duration of 0.2 ms [KKT02]. There are also other sensory substitution systems which employ the combination of electrotactile and vibrotactile displays [KWByRT91]. Although these systems are simple and can be easily controlled, it is challenging to achieve good comfort level, optimum spatial resolution and low power consumption.

3.2 Vibrotactile Actuators

Vibrotactile actuators are the most widely researched and developed actuators, because the vibrations are easily sensed by mechanoreceptors when compared to other kinds of mechanical stimuli. The different types of vibrotactile actuators that are used in tactile displays are:

- Rotary DC motor
- Linear resonant actuator
- Piezoelectric actuator
- Electroactive polymer
- Shape memory alloy
- Carbon nanotube

3.2.1 Rotary DC Motor

Eccentric Rotary motors (ERM) are one of the most commonly used vibration actuators, and they are used in toys, joysticks and virtual reality tactile devices. In these

motors, there is an off-centered mass (eccentric mass) that is fixed to the output shaft of the motor. When DC current is applied, the motor rotates and this off-centered mass provides vibration see Figure 3.1. A large applied voltage leads to strong and fast vibration whereas a small voltage creates slow vibration, which means that the strength of vibration varies linearly with the voltage and current applied [BN99].

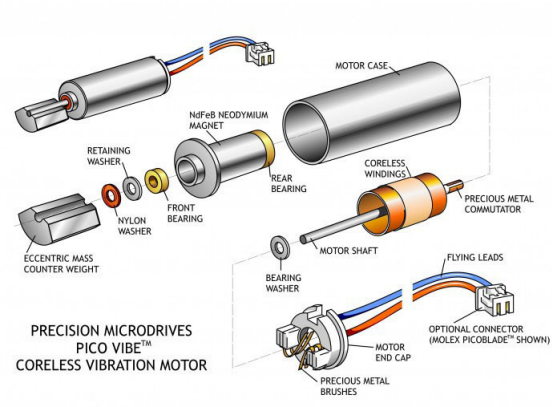

FIGURE 3.1: Eccentric Rotating Mass Vibration Motor. Image Source: [Mic19a]

Though there are some benefits of using this type of actuator such as cost-effectiveness, easy setup and relatively strong vibration, they have some important drawbacks. They are not suitable for high precision tactile feedback because the rotation generated is non-directional. In addition, they are a poor candidate for high-resolution feedback systems as their size is relatively large. Also, the other drawback includes slower response time, in the range of tens of milliseconds.

3.2.2 Linear Resonant Actuator

Linear Resonant Actuator (LRA) generate vibrations using electromagnetic inputs. These actuators use AC signal as input to drive a voice coil connected to a moving mass through a spring as shown in Figure 3.2. As the voice coil moves the magnetic mass against the spring, the entire actuator is displaced to cause vibration. The voice coil inside the housing remains stationary and it uses the magnetic field to produce force. Since LRAs use AC current, the amplitude and frequency of vibration can be modified independently. These actuators work best when the input frequency is equal to the resonance frequency of the system.

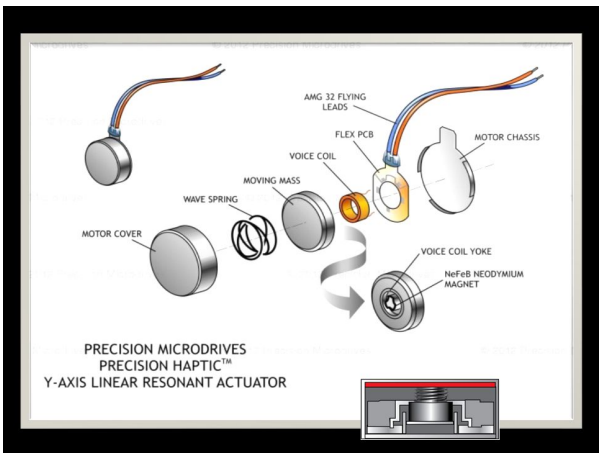

FIGURE 3.2: Linear Resonant Actuator. Image Source [Mic19b]

LRAs have faster reaction times than rotary motors, but it is still slow for a fast response tactile system. These actuators are mostly used in mobile phones because of their compact size and low cost.

3.2.3 Piezoelectric Actuator

A piezo actuator bends or deforms when a differential voltage is applied across both ends of the actuator. The current consumption in a piezoelectric actuator is low, even though it needs higher input voltages than inertial actuators. Multi-layer piezos can also be used to provide a stronger haptic response and a better localized feedback. [XLY+17]. Figure 3.3 shows the schematic diagram of piezoelectric effect.

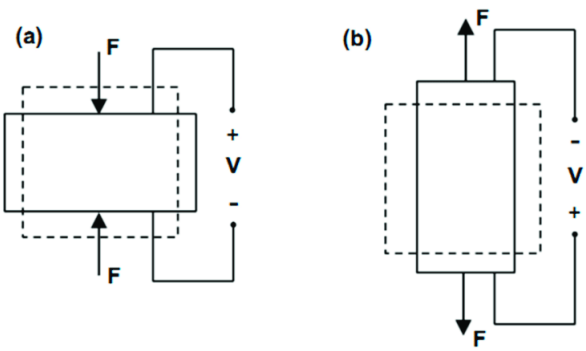

FIGURE 3.3: Schematic diagram showing piezoelectric effect, which is reversible. The dashed line represent the original shape, solid line represents the deformed shape. Adapted from [MUNM19]

Piezoelectric materials such as piezoelectric polymers, like polyvinylidene fluoride (PVDF) and piezoelectric ceramics like lead zirconate titanate (PZT) are some of the commonly used materials. The relationship between the voltage applied and the mechanical deformation is called piezoelectric coefficient d, which is defined as:

$$d = \frac{strain\ developed}{applied\ electric\ field} \tag{3.1}$$

Piezoelectric materials respond very quickly (microseconds) to electrical stimuli and are often used to produce high frequency vibration. As the process of changing its shape is reversible, piezoelectric materials are often used to detect the force applied on the material or corresponding mechanical deformation in sensors.

3.2.4 Electroactive Polymer

Electroactive polymers (EAP) are a group of polymers that change their size and shape when electric voltage is applied, resulting in vibration. These actuators are small with a pitch of just few millimeters and they can provide millimeter-scale actuation, with actuation times on the order of tenths of seconds [BC09]. Dielectric elastomer actuator (DEA) are a type of EAP, which are based on electromechanical response of a dielectric elastomer film sandwiched between two electrodes. The electrostatic pressure compresses the film when voltage is applied and reduces the thickness. Therefore, the electrode film is forced to expand in the planar direction. These unique bending characteristics also allow them to mimic biological movements of muscles and limbs. Figure 3.4 shows the principle of operation of a DEA.

EAP require voltages higher than 300V to function effectively, which is not ideal for portable tactile devices. In addition, EAP is robust, but has slow refresh rate.

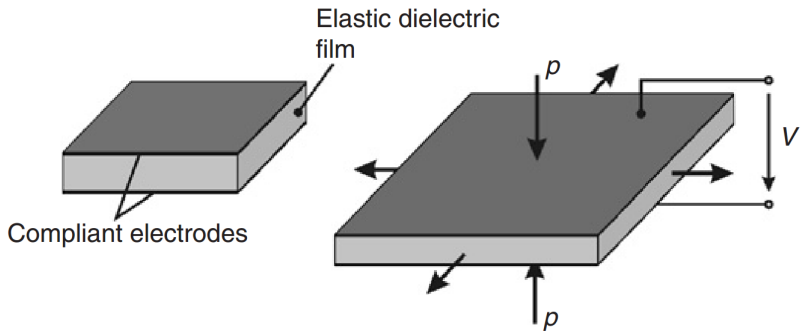

FIGURE 3.4: When voltage is applied, polymer film compresses in thickness. Adapted from [ZKK+04]

3.2.5 Shape Memory Alloy

Shape Memory Alloy (SMA) have the ability to change their shape when subjected to temperature changes because they exhibit different phases of solid at different temperatures. An SMA actuator of wire-type can be considered very effective due to its high power-to-weight and force-to-volume ratio. But unfortunately, their long relaxation time is a disadvantage for some feedback tasks. In addition, their large power consumption also makes it impossible to use SMA in real-time vibrational tactile display. The most common SMAs available are NiTi (Nickel titanium) or copper-based alloys. [MMT+05, MEBA15]

3.2.6 Carbon Nanotube

Carbon Nanotube (CNT) is a smart material similar to EAP and SMA, which is used to provide tactile sensation. One of the first demonstration of these electromechanical actuators by Baughman, *et. al* was based on single-walled CNTs for various applications, such as temperature insensitive material (jet engines) and micro-cantilevers for medical catheters [BCZ+99]. Lima, *et al.* demonstrated CNT artificial muscles that are strong and fast. They are powered by photonically and electrically activated guests [LLDA+12]. Due to the ultra strong C - C bond in CNTs, they have some really good thermal, mechanical (10 fold strength vs carbon fiber) and electric (current density is 1000 times higher than copper) conducting properties. These materials can also be fabricated into different shapes and sizes with high aspect ratio and good

stability, making them an ideal candidate for high performance tactile applications [LZZ+12].

Recently, few other approaches have been made by adapting the use of multi-walled carbon nanotubes (MWCNTs) with high mechanical strength and high conductivity, and CNT-PDMS composite tactile sensors with low-cost batch production capabilities. Caamargo, *et al.* [CTC+11] demonstrated an optically powered tactile sensor by activating Braille dots made from liquid crystal - carbon nanotube (LC-CNT) composite as seen in Figure 3.5.

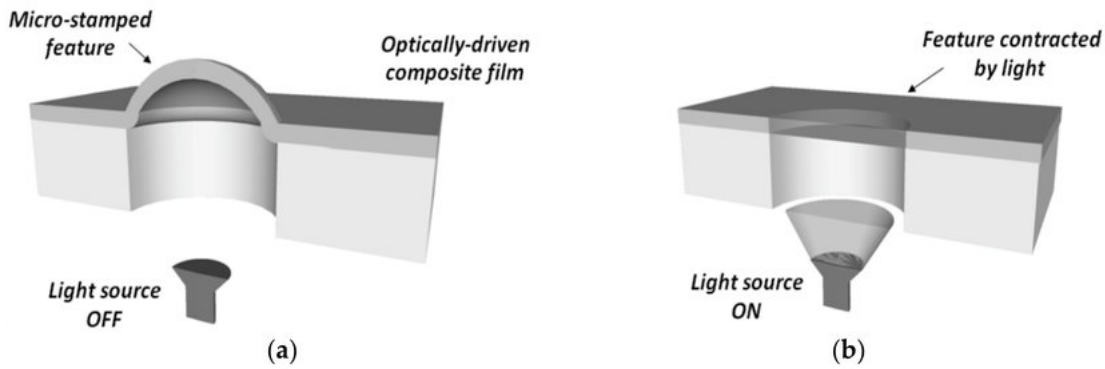

FIGURE 3.5: Schematic concept of carbon nanotube (CNT) composite film driven by the light source. (a) Default state: light source is OFF. The feature is micro-stamped and high-relief dot (b) feature is contracted when light source is ON. Adapted from [CTC+11]

3.3 Discussion

In this chapter, various tactile actuation technologies based on their application in the field of haptics, and their advantages and disadvantages are discussed. It is important to choose an actuator to provide tactile feedback based on their feedback effectiveness, power consumption, cost, complexity and other factors as shown in Table 3.1.

Based on compactness and system complexity, the choices were narrowed down from 7 actuators to 3 actuators. The 3 actuators decided were ERM, LRA and piezoelectric actuators. The next deciding factors were response and durability. Based on these two factors, the ERM were not a good fit. So, the choice was between LRA and

piezoelectric actuators. Though the feedback effectiveness and power efficiency of the piezoelectric actuators were much superior to the LRAs, cost was a major deciding factor and LRAs were chosen for this thesis. Also, piezos require driving signal at a relatively high voltage up to about 200 V.

TABLE 3.1: Comparison of different vibrotactile actuators

Actuator Technology	Feedback Effectiveness	System Complexity	Size (mm)	Power Efficiency	Response	Cost	Durability
ERM	-	++	11x4.5 dia	-	- ($\sim 50ms$)	++ (2-3€)	-
LRA	+	+	10x3.6	+	+ ($\sim 30ms$)	++ ($\sim$5€)	+
Piezoelectric	++	+	3.5x3.5 x42	++	++ (<5ms)	- ($\sim$60€)	+
DEA	++	+	45x38x 0.8	-	+ (<20ms)	- ($\sim$40€)	++
SMA	+	-	15x4x 0.95	-	-	+ ($\sim$15€)	+
ETS	+	++	o	++	++	++ ($\sim$10€)	+
CNT	++	+	–	+	-	-	+

In LRAs, both frequency and amplitude of vibration can be manipulated independently by changing the AC voltage input. They are ideal for operating in specific frequency range as they effectively work at narrow resonance frequency. They are a good alternative to ERM motors as they can generate higher frequency vibration (eg. 175-250 Hz) close to the frequency of the skin. The LRA also has an advantage in terms of fast response speed and efficient energy storage and hence, enhanced haptic performance. They are a better candidate for sharp and crisp vibrational feedback with better start and braking characteristics when the voltage is changed. [PCH+11]

Actuators provide tactile feedback which helps in interacting with virtual objects. By choosing LRA as the actuator instead of ERM, the energy consumption has been reduced due to the greater efficiency of the LRAs. When compared to piezoelectric actuators, the LRAs operate at a lower voltage, thereby reducing the running cost. As tactile stimulation provided by the actuator is the main function of the

device, choosing an actuator is very important as it affects the implementation the entire system. The choice of hardware components and mechanical design which are discussed in Chapters 4 and 6, are also based on the choice of the actuator.

Further research on these micro actuators is very important as they have to be developed economically with less complexity. The research on these actuators will be beneficial for using them not only to assist people to perceive their environment, but also for providing force and motion in microrobotics, and advance actuation in virtual or augmented reality. Suggested research will also investigate how to close the gap between macroscale forces and micro components at the MEMS scale to create effective tactile stimuli. MEMS actuators are small, outputting adequate force and displacement, and can surely help tackle the challenges to provide high-resolution tactile actuation.

Chapter 4

Design Guidelines and Hardware Setup

Wearable haptic devices allow application of actuation and sensing to different areas of the body. While the major focus of this thesis is finger-related haptics which naturally deals with interactions by manipulation and grasping tasks, wearability of the device can lend towards the feedback applied on the surface of the fingertips. In this chapter, the guidelines to design a wearable device is first discussed. Then, the hardware components required to complete the required tasks are explored.

4.1 Design Guidelines

Some of the existing devices discussed in Chapter 2 are sometimes acceptable in VEs but they are not the best choice for AR. This is because, in an AR environment, the user interacts with both the virtual and real objects, and it is important to not obstruct the user from using their fingertips to interact with the real environment. Therefore, it is important to discuss the target guidelines that define the wearability of a tactile device. Table 4.1 summarizes the target guidelines to design wearable devices.

- *Weight* - The weight of a haptic interface device is comparable to the strength of the skeletal support on which it is used. This makes the absolute weight of the device sometimes misleading. For example, a device may be lightweight when worn on the leg and becomes heavy when worn on the forearm. For

applications in most cases, a lightweight device causes less fatigue and is intuitively more comfortable than a heavy device.

TABLE 4.1: Target Guidelines for Design of Wearable Devices.

Weight	Wearable devices should not be heavy and cause fatigue to the user.
Comfort	Wearable devices should easily adapt to the finger's shape and size, and should be comfortable.
Form Factor	Wearable devices should not alter the body size of the user in any way.
Impairment	Wearable devices should not limit the motion of its user wearing the device.

- *Comfort* - A wearable fingertip tactile device should be comfortable and easily adaptable to the user's finger. Often, wearing a device for long periods can result in major discomfort and in most cases, it is also related to the weight of the device. This is due to the pressure exerted by the device worn on the finger. Discomfort is also caused because the haptic devices have to be fastened tightly to transfer tactile cues at the points of stimulation. In regards to adaptability, it is also important to consider the variability in size and shape of human body parts, including the finger [BAG92]. So a wearable interface should be designed to accommodate different finger sizes. Also, when designing the actuator responsible for tactile actuation, the type of actuator and their high torques are also important considerations for comfort. For example, electrotactile stimulation with small electrodes that generate high current densities can cause discomfort. Therefore, a proper design should incorporate the position and placement of the end-effectors which are in contact with the skin, to establish a better tactile feedback.

- *Form Factor* - Form factor is an important target objective when evaluating the wearability of a device. Though compact devices are instinctively more wearable, the absolute form factor of these devices should be compared to the body part it is attached to. The device should be designed and shaped to fit the respective body part and should not get in the way of its natural movement. This employs for a smooth design of the device to fit most of the shapes and sizes of the human body.

In haptic devices, actuators which provide feedback information are usually bulky and heavy. This is particularly challenging for a finger-mounted device, because the amount of force a finger can exert with respect to its size is higher than any other limb [MAB+19]. This is different in kinesthetic devices as they have to allow free active motion of the user than compared to fingertip devices, where the movement of the finger is not obstructed as they act on the fingertip irrespective of the actuation system. It is precisely for this reason, we chose to use LRAs as actuators to provide tactile stimulation's due to its compact form factor.

- *Impairment* - According to [ZP12], there are 230 joints in a human body which are controlled by 630 skeletal muscles. This sums to a total of 244 degrees of freedom for a human being. For this reason, impairment caused by a haptic device is an important factor, so that a wearable device ensures correct kinematic compatibility with the human body and fits naturally without impairing any actions. The devices should also be able to function without any additional voluntary action [GKS+98]. In our design, the device should employ a configuration that minimizes interference with the finger-pad, so that the user can also interact with real objects.

4.2 Hardware components

In this section, we will discuss the physical hardware components that were necessary to develop our tactile device: what components do we need, why and what are the specifications of these components.

The tasks the hardware components have to complete are:

- to provide adequate and correctly oriented tactile feedback to the finger
- to navigate through AR by detecting the objects in real environment.
- to alter the incoming amplitude and frequency of vibration to output different tactile feedback patterns.

In order to accomplish these functionality requirements, the important hardware devices used are a IoT microcontroller, a time of flight (ToF) sensor and a motor driver.

4.2.1 Microcontroller

The microcontroller is the most crucial part of the device, as it is responsible for making sure that the measurement data from the sensor is received and based on this, the actuators receive instructions from the external processor (motor driver). It is equipped with a central processing unit CPU, an input/output system, a memory system, a clock system and a bus system to interconnect essential components. The microcontroller will act as a tiny computer, when implemented on the user's wrist. As there are many microcontroller to choose from in the market, it is often difficult to choose one. For implementing wireless connection between the hardware in future, ESP32 was chosen as the microcontroller during this thesis (see Figure 4.1) . It has a wide selection of GPIO pins with high clock frequency of the CPU. Also, it is a low-cost and a low-power system with dual-mode Bluetooth and Wi-Fi capabilities.

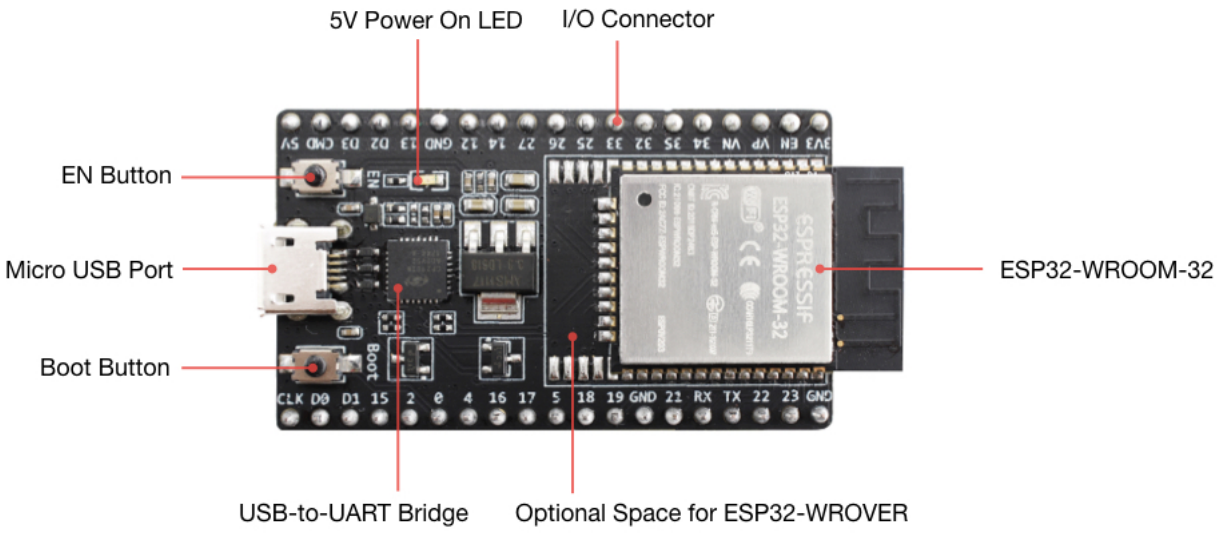

FIGURE 4.1: ESP32 Development Kit. Image Source: [Esp19a]

Along with ESP32, Espressif Systems also offers ESP-WROOM-32, which is a small size and easy to use IoT module often used for prototypes and tests. Some of the other characteristics of ESP32 compared to other popular microcontrollers are mentioned in Table 4.2.

TABLE 4.2: Hardware Selection: Microcontroller. Input from [Esp19a, Esp19b]

	ESP8266	ESP32 (ESP-WROOM-32)	CC32 CC3220MODSF	Xbee (XB2B-WFPS-001)
Size (*mm*)	24.0 x 16.0 x 3.0	25.5 x 18.0 x 2.8	20.5 x 17.5 x 2.5	24.0 x 22.0 x 3.0
Cost	8 €	12 €	20 €	30 €
SRAM	36 KB	520 KB	256 KB	N/A
Work voltage	3.0V - 3.6V	2.2 - 3.6V	2.3V - 3.6V	3.14V - 3.46V
Clock	80M*Hz*	80M*Hz*	80M*Hz*	N/A
Open source	Yes	Yes	No	No
I/O:				
GPIO #	17	32	21	10
ADC	1 (10-bit)	18 (12-bit)	4 (12-bit)	4 (12-bit)
DAC	-	2 (8-bit)	-	-
I2C	1	2	1	-
Connectivity:				
Wi-Fi	802.11 b/g/n	802.11 b/g/n	802.11 b/g/n	802.11 b/g/n
Bluetooth	-	4.2 BR/EDR + BLE	-	-
UART	2	3	2	1

4.2.2 Distance Measurement

During the use of the tactile device in Augmented Reality, we need a way to determine the proximity of the real object in real time. There are several ways to detect the distance that incorporates extremely broad field of technologies such as laser, Infrared (IR) triangulation, ultrasonic and Time-of-Flight. ToF sensors are compact, easy to use and lightweight, which are important requirements for our device. They also support rapid refresh rates for precise distance measurements and multi-sensor integration. Compared to ultrasound sensors, which are also quite compact, ToF sensors provide greater accuracy and faster readings while still maintaining low weight, small size and low power consumption. [Jar83]

The main advantages of a ToF sensor are:

- The sensor is very compact.
- The technology provides very accurate results and is very easy to use.
- It can also work in low light conditions.
- The reflectance of the object does not have any influence on the measurement.
- It is capable of measurements in real-time.

The principle of a ToF Sensor is based on computing the time a light pulse takes to travel from sensor to the target and back. The time of flight is the time it takes for the pulse to travel from an emitter to the target and then back to a receiver. The distance is measured as:

$$distance = \frac{1}{2}c\tau \tag{4.1}$$

where c is the speed of light and τ is the time of flight.

To detect the phase shift between the illumination and reflection, the light source from the sensor is either pulse or continuous wave, i.e., square or sinusoidal wave. The most commonly used modulation is square wave as it can easily be realized by digital circuits. Figure 4.2 shows the basic working principle of a ToF sensor.

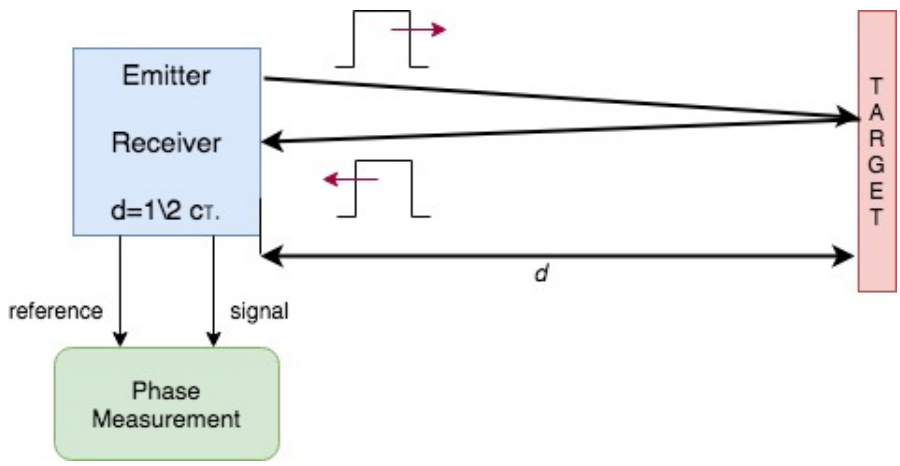

FIGURE 4.2: Basic principle of a ToF sensor. Adapted from [KRI06]

Flightsense is a technology patented by STM Electronics and it solves some of the issues such as the reflectance caused by the glass covering of the sensor. There is a compensation algorithm for correcting this distortion as the glass has fixed optical properties and is located at the same place. Another improvement is in the outdoor performance because sometimes, the high intensity light can saturate the sensor. This technology, with time-domain rejection and optical filtering, rejects the ambient and lower wavelength photons enabling better accuracy. There are wide range of products that use this technology and for our proximity range, VL6180x is a good candidate. This sensor along with an IR emitter, also combines a range sensor and an ambient light sensor that helps to work accurately in ultra low-light conditions. It is a low-power, low-cost and easy to integrate ToF sensor. It is controlled using I2C (Inter Integrated Circuit) communication protocol, which offers a possibility of sending back data to the master device (the Microcontroller) and connecting it alongside other I2C slave devices such as, the motor drivers. [STM19b]

The Application Protocol Interface (API) for this sensor allows us to collect the proximity data with two ranging modes: single shot and continuous. Due to these two ranging modes, We will be able to use 3 different operating modes in the sensor.

- Single Shot - Polling mode: The master device will send a signal for single measurement and then wait for the sensor or the slave to send back the result. This mode is easy to use but CPU is always busy, which lease to more power use.

- Single Shot - Asynchronous mode: The master device requests a single shot measurement and regularly check if the result is ready or not. This is mostly used in systems where CPU is synchronized by a timer.

- Continuous - Interrupt mode: Here, the sensor is continuously sending results to the master device, which is also waiting for interrupts along with the results of measurements. This mode helps to save power, as the CPU is free or asleep during ranging when no target is detected within the proximity range by the sensor.

The sensor has a single-photon avalanche diode (SPAD) photodetector array, which detects single photons with picoseconds resolution that is usually used to measure targets at close distances. It incorporates a tiny laser source, a 850 *nm* VC-SEL for emitting the light pulse with a focused direction and stable wave-length. The sensor is capable of measuring distance up to 100 *mm* and with good ambient conditions, up to 150-200 *mm*. For a tactile device in AR, this close range sensor is very convenient to interact with the real environment. Figure 4.3 shows VL6180x sensor on a breakout board equipped with regulator and level shifting, which measures only 20x18x3mm.

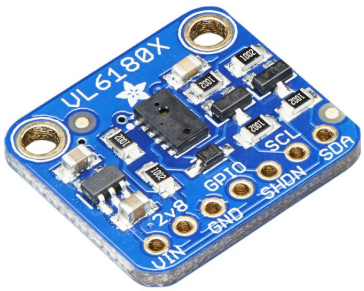

FIGURE 4.3: Adafruit VL6180x ToF sensor

4.2.3 Vibrational Actuators

The third component are the LRAs used to provide vibrational tactile feedback on the finger. As discussed in the Chapter 3, after investigating different actuators, we came to a conclusion that LRA is a good candidate for our application. It has several advantages like longer lifespan, low power consumption, compact size, short lags and complex waveforms, which can essentially produce a richer haptic experience.

LRA actuator uses electric current and magnetic field to product force. The mass-spring system in an LRA acts as a simple harmonic oscillator displaying resonance, which means that the device oscillates at higher amplitudes at particular frequencies. So in order to product a useful amplitude of vibration, the frequency of the input signal must match the resonant frequency of the spring. The amplitude increases linearly with increasing voltage while the frequency remains fixed. LRA requires an AC signal to drive the magnetic mass and this requires a dedicated motor driver.

However, LRAs are designed to be very efficient [Mic19b]. Both the energy loss and the bandwidth are described by quality factor or Q and higher Q value indicate a very narrow bandwidth but very low energy loss. Datasheets of LRAs indicate resonance frequency ranging from 175-235 *Hz*, and the limit being 250 *Hz*.

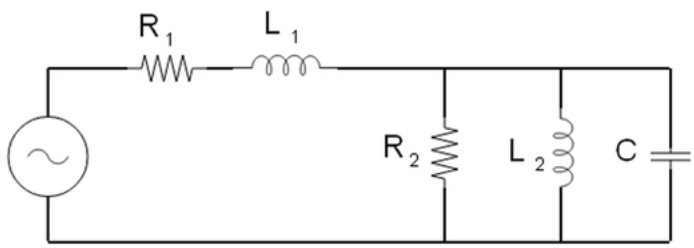

FIGURE 4.4: LRA Equivalent Circuit. Source: [**?**]

The LRA fits the mass-spring-damper one DOF model perfectly, and its equivalent electric circuit is shown in 4.4. Capacitor C, Resistor R_2 and Inductor L_2 in parallel represent the impedance of the mechanical section, as the magnetic mass oscillates. The overall impedance of the parallel circuit is given as:

$$\frac{1}{Z_{tot}} = \frac{1}{Z_C} + \frac{1}{Z_{R2}} + \frac{1}{Z_{L2}} \tag{4.2}$$

where,

$$Z_C = \frac{1}{j\omega C},\ Z_{R2} = R,\ Z_{L2} = j\omega L \tag{4.3}$$

In Equation. 4.2, ω is the frequency. It can be seen that the impedance of the capacitor decreases at higher frequencies, while that of the inductor increases. This means that, at a specific frequency, the impedance's balance out to make the total impedance Z_{tot} maximum. This leads to a drop in voltage and the mass oscillates at greater force. This frequency is called resonant frequency. The LRA used in our prototype is ELV1036, which is a y-axis linear vibrator and vibrates perpendicular to the mounting plane. Table 4.3 shows some of the important specifications of this actuator.

TABLE 4.3: ELV1036 LRA specifications. [NFPMC19]

Model	NFP - ELV1036AS
Vibe Force	1.8 G
Dimensions	dia 10 x 3 mm
Rated Voltage	AC 2.0 V_{rms}
Rated Operating Current	75 mA
Resonant Frequency	205± 5 Hz
Cost	5 €

4.2.4 Motor Driver

The final component that is used is the motor driver which acts as an interface between the actuator and the microcontroller. The function of the motor driver is to turn the low-current control signal into a high-current control signal to drive the motor. In AR, when detecting objects at different distances, the vibrating characteristics should also change in a manner that the user can recognize. This implies that the vibration must convey more information with different vibration amplitudes and patterns than just a simple on/off alert. Different vibration waveforms will provide different patterns and to obtain this, the following techniques are required from a motor driver.

- Active braking: To have a crisper vibration feedback, the actuator must be quickly stop when the current flow is stopped. In most cases, due to the momentum of the actuator, the vibration slowly fades away after a few milliseconds. To improve this, the AC signal can be switched 180° out of phase.

- Overdrive: Overdrive supports any quick jumps in vibration intensity and improves responsiveness. This is achieved by applying a voltage higher than the actuator's rated voltage for a short time period, but not exceeding the maximum operating voltage. There is a stronger magnetic field due to higher voltage, which in turn increases the acceleration of the internal magnetic mass.

Texas Instruments have produced motor drivers especially for haptics that utilise these techniques and one of their drivers (DRv2605) is used to drive the LRAs in

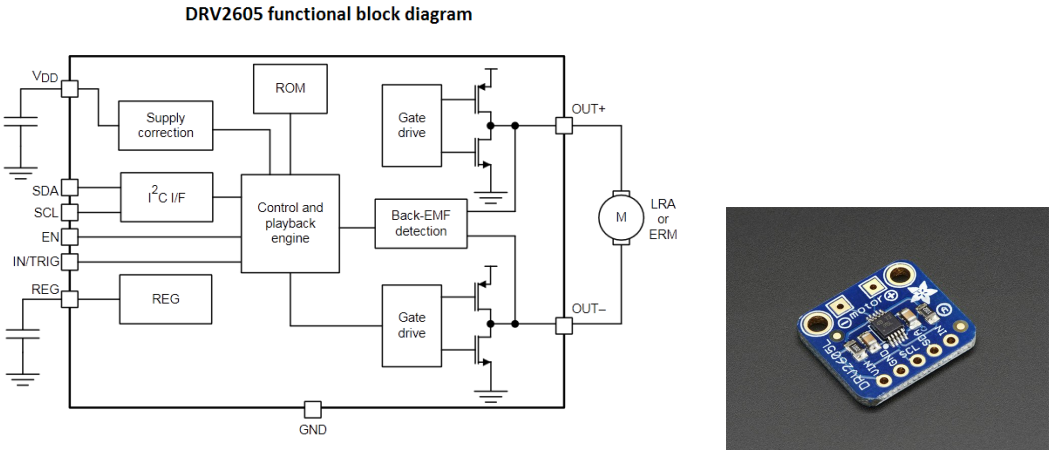

(A) DRV2605 Driver Functional Block Diagram (B) Adafruit DRV2605 board

FIGURE 4.5: Motor driver DRV2605. Source: [Ada19]

our device. It is produced on a small enough breakout board by Adafruit to fit our specifications for a wearable device (see Figure 4.5b). It allows detailed and precise vibrations with the help of smart-loop architecture and it uses I2C communication bus, which will also help us easily integrate the driver to the microcontroller along with other slave devices. The functional block diagram of DRV2605 is shown in Figure 4.5a.

Since the address of DRV2605 cannot be changed and it can drive only one actuator at a time, two DRV2605 motor drivers are used to drive two LRAs. DRV2605 also has a auto resonance tracking feature, which means it will always drive the signal to match the resonant frequency, irrespective of the mounting surface. It also has an in-built library with different vibration effects such as clicks, ramps and buzzes. These are mostly used for creating notifications and alerts, but are not suitable for biorhythmic patterns. Rather, PWM input signals are used to create our own effects, which can accurately control haptic strength and duration.

4.3 Chapter Summary

The wearability of haptic interfaces has extended the scope of haptic technologies. In this chapter, the important guidelines that are required to design a wearable fingertip tactile device were discussed. The guidelines are important not only for the

physical design, but also to select the hardware components, as they are directly influenced by these target guidelines like weight, comfort, form factor and impairment. The main component is the microcontroller used as a controlling device that executes programs to control other slave devices. Based on our requirements, ESP32 was chosen, which is a small and powerful microcontroller. The other main components implemented are the ToF sensor and the motor driver, which are used to measure distance to real objects in AR and drive the actuator respectively. The ToF sensor, VL6180X, is a very compact and easy to use sensor accurate at close distances. This makes it possible to easily gauge the object distances and interact with the environment easily. DRV2605 is the motor driver that selected to drive the LRAs and also obtain different vibration patterns. The driver also employs techniques such as active braking and overdrive for crisp vibrations. As LRA relies on AC voltage to drive the mass, DRV2605 is used with a PWM input signal and duty cycle to change the amplitude of vibration, and output different vibration patterns.

Chapter 5 details the hardware integration of the different hardware components selected and the implementation of software to execute different tasks to produce vibrotactile actuation.

Chapter 5

System Implementation

Chapter 4 provided an overview of the required guidelines to design a wearable tactile device and the hardware components to develop a functional prototype. The prototype developed consists of four main hardware components: ESP32 Microcontroller, ToF sensor, Motor driver and LRAs.

In this chapter, the above considerations are extablised into a specific design by implementing the software and the decisions made during the software development process are illustrated. Also, the complete integration of hardware components to drive the actuator based on the measurement from the ToF sensor is discussed.

5.1 Software Development

The Software development section is divided into two parts - proximity sensing with the ToF sensor and vibration pattern generation with DRV2605. The development environment used is Arduino IDE, which is a cross platform written in functions from C and C++. It is an open-source prototyping platform for rapid prototyping of embedded systems and wearable applications. It also supports wireless data transfers, such as over Wi-Fi or Bluetooth and deployment of code to the microcontroller is quite streamlined.

5.1.1 ToF Sensor Interface

As discussed in Chapter 4, ToF sensors are one of the most suitable sensors to measure the distance to various objects in close proximity. VL6180X breakout board from Adafruit is used, which has an onboard 2.8 V regulator. This means that if voltage greater than 2.8 V is sent, it will automatically shift down the voltage without damaging the board.

VL6180X uses I2C communication protocol, which means it uses two lines to communicate with the master device (microcontroller). SDA or Serial data is used to send and receive data between the master and the slave. SCL or Serial Clock carries the clock signal. The information is packed in an 8-bit packet followed by an acknowledge bit, and the data is transferred bit by bit along the SDA line.

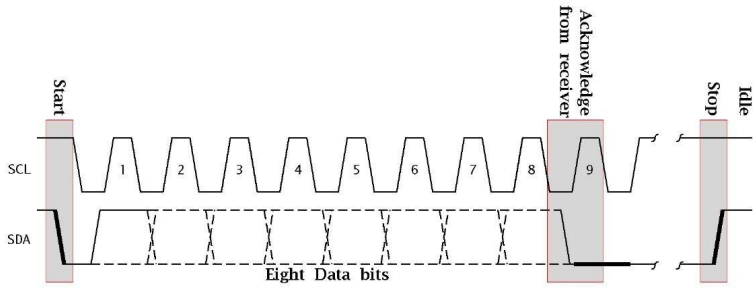

FIGURE 5.1: I2C data transfer protocol. Adapted from [HDCD11]

The data transfer protocol of an I2C bus is shown in Figure 5.1. After the start condition, the first 8 bit sequence which indicates the slave address, is sent to the slave(s). The acknowledge bit follows this 8-bit sequence and then, the address for the internal registers of the slave devices are sent. After this addressing sequence, there is one of multiple 8-bit data sequences until the data is completely sent and the stop condition is called.

Figure 5.2 shows the pinout configuration of VL6180X. *Vin* and *GND* have to be connected with voltage level between 3-5V and common ground respectively. The I2C wires SDA and SCL are connected to the I2C pins on the Microcontroller, in our case, to GPIO pins 21 and 22 respectively (see Figure 5.6) .

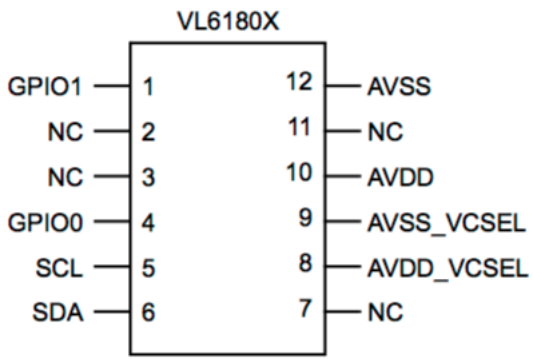

FIGURE 5.2: VL6180X pinout diagram. Source: [STM19a]

The source code is based on the example code provided by the supplier of the sensor. The operation mode of the VL6180X sensor can be set by writing into different chip registers, which can be found in the datasheet [STM19a]. The sensor is initialized and an absolute range reading is obtained by reading the register *RANGE_VAL*, which returns the actual range in mm. Because the maximum operating frequency is 400 *Hz*, a timer is implemented to update the value frequently. The code for the read function is mentioned below:

```
void VL6180X_Read() {
  int range;
  WriteByte(RANGE_START,0x03); %0x01 for single shot mode
  if (! (read8(INTERRUPT_STATUS) & 0x04))
  range = ReadByte(RANGE_VAL) %Read Range in mm
  WriteByte(INTERRUPT_CLEAR,0x07);%clear all interrupts
  Serial.println(range);  %Print range value
  return range;
}
\label{list:5.2}
```

LISTING 5.1: VL6180x - Range Reading

For single-shot mode, the register *RANGE_START* (0x018) should be set to *0x01*. All the register addresses and functions which are relevant to our data collection are declared in the header file (.h) found in Appendix A.

5.1.2 Motor Driver Interface

LRA is used to provide tactile stimulation at the fingertip and to drive these LRAs, the motor driver DRV2605 is implemented. It is designed to provide extremely flexible haptic control of LRA actuators over I2C communication protocol.

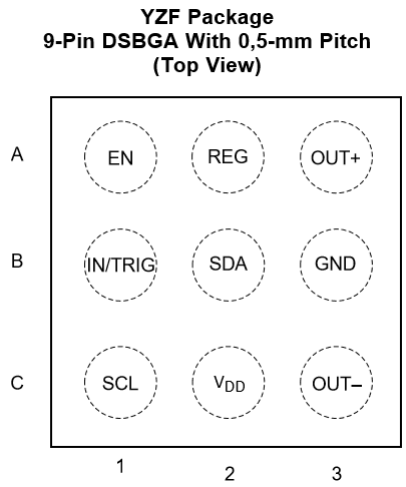

FIGURE 5.3: DRV2605 Pin Configuration.
Source: [Ada19]

The driver relies on the back-EMF that is produced by the actuator to provide a closed loop system. This increases the actuator performance in terms of the start time, brake time and acceleration consistency. It also has a PWM interface mode with the control range of 0 - 100%. The pin configuration of DRV2605 is shown in Figure 5.3. The breakout board from Adafruit consists of a voltage regulator and a 0.1 µF capacitor. This allows us to give the same power to the board as the logic level on the ESP32, which is 3.3 V. The SDA and SCL pins also have 10K pullup resistors, to provide a default start to the signal line and restore the signal back to high level. Table 5.1 describes the pin functions of DRV2605.

TABLE 5.1: DRV2605 Pin Functions

Pin	Description
VDD	Supply input to power DRV2605 (2.2-5.5 V)
GND	Supply ground
IN/TRIG	multi-mode signal input, PWM or analog
OUT+	Positive motor differential output
OUT-	Negative motor differential output
SDA	I2C Data
SCL	I2C Clock

The supply input pin *VDD* is connected to the power supply of 3.3 *V*. The SDA and SCL lines are connected to the corresponding I2C pins on the ESP32, i.e., GPIO pins 21 and 22 respectively. The driver accepts PWM data from the master device at IN/TRIG pin, when driving in the PWM interface mode. The actuator is continuously driven in the PWM interface mode till the user sets another interface or standby mode. In standby mode, duty cycle determines the strength of vibration. Figure 5.4 shows the standard wiring diagram for typical haptic implementation using a PWM interface.

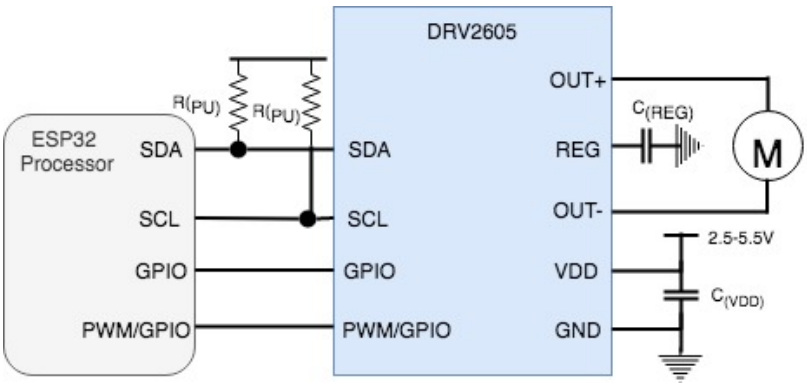

FIGURE 5.4: I2C Wiring with PWM Input Interface using DRv2605.

Pulse-width-modulation or PWM, which means switching the current on and off in rapid succession, is an effective way to control the actuator. The ratio of on-off times define the effective voltage supplied to the motor, which in turn controls the strength of vibration. The internal PWM generator of the microcontroller allows values from 0 to 255, where the maximum value corresponds to approximately 4*V*. At this voltage, the motor reaches its peak vibration strength and frequency average of about 210 *Hz*. The specifications of different registers and their addresses are taken from the Datasheet [Ada19] and an Arduino class is generated combining all the relevant functions of the driver. The initialization function used to initialize the motor driver can be found in Appendix A. The bits in the control registers are responsible for reducing the actuator brake-time performance, improve brake stability and increasing back-EMF gain. Higher values on these prove less-stable operation but the default values should provide really good performance for most actuators.

The optimum drive time for an LRA can also be set using the *CONTROL1* register, which is given as:

$$\begin{aligned} Optimum\ drive\ time\ (ms) &= 0.5 * LRA\ Period \\ &= \frac{0.5}{205\ Hz} = 2.4ms \end{aligned} \tag{5.1}$$

The optimum drive for an LRA with resonant frequency of 205 *Hz* is approximately 2.4 ms. The header file (.h) containing all the relevant registers and functions can be found in Appendix A. As mentioned earlier in Chapter 4, DRV2605 contains smart loop architecture, which includes an Automatic Level Calibration feature. The driver has the capability to monitor the back-EMF behaviour of the actuator, as the level of back-EMF voltage varies across different actuators based on mechanical construction. This feature compensates for this variation and allows the output level to increase above the rated voltage for automatic overdrive and braking, without allowing it to exceed the specified overdrive clamp voltage. The function which defines the auto-calibration procedure settings is mentioned below:

```
void motor_autocal() {
 _wire->begin();
  writeRegister8(MODE, 0x07); %Set to autocal mode
  writeRegister8(RATED_V, 0x03);  %2Vrms   writeRegister8(
   CLAMP_V, 0xA0);  %2.82 Vpeak
  %Set default LRA drive time and sampling time
  writeRegister8(REG_GO, 0x01)    %Start auto cal %read and
   store values to EEPROM
  uint8_t ACalComp = readRegister8(CAL_COMP);   uint8_t ACalBEMF
    = readRegister8(CAL_EMP);
  uint8_t BEMFGain = readRegister8(FEEDBACK & 0x03);
}
```

LISTING 5.2: DRV2605 - Auto-calibration procedure for LRA

The value stored in the register *CAL_COMP* compensates for resistive losses in the driver and register *CAL_EMF* is the back-EMF voltage level of the actuator when

driven at the rated voltage. With these values, the appropriate feedback coefficient and feedback gain is determined by the the driver during playback, allowing for better response time and acceleration.

5.2 Arduino Integration

The next step is to integrate the ToF sensor and LRA to provide vibrational feedback based on the readings from the distance sensor. The motor driver DRV2605 is also now calibrated to drive the actuators efficiently with:

- Stronger vibrations operating at resonant frequency
- Low power consumption with auto resonance
- Overdrive and braking provides crisp vibrations

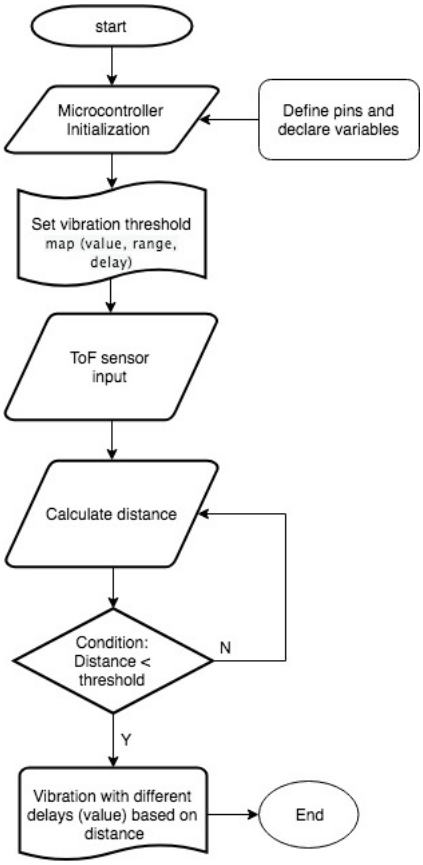

FIGURE 5.5: Flowchart of the proposed prototype.

To provide an intuitive feedback, the actuators vibrate inversely to the object distance, i.e., closer to the object, the higher the frequency of vibration. The ToF sensor VL6180x has a narrow field of view (approximately $\pm 12.5°$), but it is very precise without any double imaging and linearity problems. Figure 5.5 shows the schematic flowchart for actuations on the finger based on the distance of an object in AR.

As mentioned, I2C protocol can be used to control multiple slave devices simultaneously by one master device. As both the ToF sensor and the motor driver have different addresses, they can be connected to the same I2C communication line. With this method, it is possible to connect up to 128 devices serially communicating with the microcontroller. The microcontroller is able to differentiate between the addresses of these two slave devices and communicate with them independently. The wiring diagram of the entire setup is shown in Figure 5.6. The *IN* pin on the DRV2605 is connected to one of the GPIO pins on ESP32 to output PWM signals.

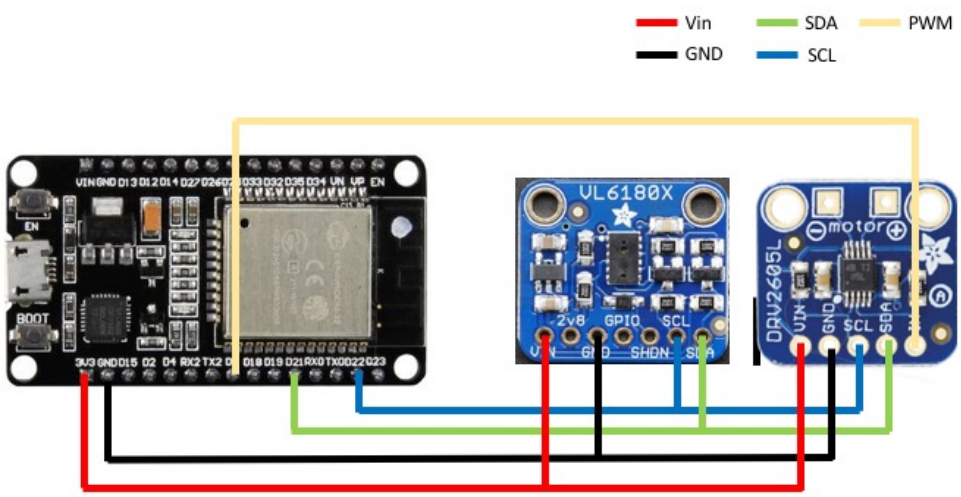

FIGURE 5.6: Circuit Diagram for Adafruit VL6180x and DRV2605 using I2C.

Following the declaration of variables and functions as discussed in Section 5.1, the serial connection between the devices is initialized as mentioned below:

```
void setup() {
Serial.begin(115200); %Initialize serial connection
 % ---------Initialize Adafruit VL6180x sensor-------------
  if (! vl6180x.begin()) {
    Serial.println("Sensor not detected \t");
    while (1);
  }
  Serial.println("Sensor Initialized!");
  % ---------Initialize Adafruit DRV2605 driver-------------
  motor.begin();
  motor.autocal();      %start auto cal
  motor.setMode(MODE_PWMANALOG); %set LRA - PWM mode
}
```

LISTING 5.3: Setup Procedure

As stated, the driver uses PWM as an input to control the voltage to the actuators. The ToF sensor reading is re-mapped to the delay time between two pulses, so that the frequency of vibration increases as the distance to the object decreases. The source code to the main loop can be structured as:

```
void loop() {
  int distance, delay;
  int delay;
  int pwmValue = 190;
  distance = vl6180x.Read();  %read the distance
  delay = map = (distance,0,250,50,300) %remap distance to delay
  if ((distance>=40) && (distance<250)){
   analogWrite(PWM_PIN, pwmValue); %
   delay(50);
   analogWrite(PWM_PIN, 0);
   delay(delay);
   }
```

```
  else if (distance < 40) {   %condition for very close
   proximity
  analogWrite(PWM_PIN, pwmValue);
}
delay(2);   %delay of 2ms for ADC to settle
```

LISTING 5.4: Read Distance value and Vibration

The distance to the object is measured by the sensor using the *READ* function, as described in Listing 5.4. Using the map function, the analog input from the sensor which takes the value between 0 to 200 is re-mapped to the values between 50 to 300. These new values represent the delay time during the off cycle of the vibration motor and is used to set the PWM frequency. The amplitude of vibration is kept constant by writing an analog value using *analogwrite()* and delay time changing to a new value depending on the measurement from the ToF sensor. Even though the PWM generator allows values between 0 and 255, where 255 corresponds to peak vibrational strength, the PWM value to 190 for pleasant vibrations. As the object gets very close and the analog reading from the sensor is below 40, the actuator vibrates without any delay. This notifies the user that the object is at a very close proximity.

5.3 Chapter Summary

In this chapter, the software development process based on the functionality of the device was discussed. The development process was initially be divided into two sections, namely, the ToF interface and the motor driver interface. The initialization and functions implemented to measure the distance and drive the actuator with different delays are also described. Lastly, the two devices are integrated together to provide vibration patterns based on the measurement from the ToF sensor.

Chapter 6

Mechanical Design

As discussed in Chapter 3, the sense of touch in humans is composed of different types of mechanoreceptors that are sensitive to modalities such as vibration and pressure. The simultaneous stimulation of these receptors enables us to interact with the virtual and real environment, through actions like touch and grasping.

This chapter presents the mechanical construction of the fingertip tactile device. As discussed, one of the subgoals of this thesis is to develop a compact and lightweight device, which provides vibrational feedback during interactions with objects in the virtual environment. First, the stimulation points on the finger are investigated to understand the location and placement of the two actuators. Then, the materials and parameters of the 3D printing process are discussed, which are important to fabricate the device. Lastly, the chapter concludes with the mechanical design based on the different requirements to build a functional prototype.

6.1 Fingertip Stimulation

Human fingertips are one of the most sensitive skin areas of a human body. Just underneath the epidermal ridges (fingerprint region) of the finger are mechanoreceptors that respond to tactile stimulation. The fingertips are also primarily involved in manipulation and grasping of objects in our environment. Due to this, there is a specific interest in the design of tactile interfaces for fingertips. The studies that have been conducted in this Thesis so far provide different guidelines to design a fingertip tactile device.

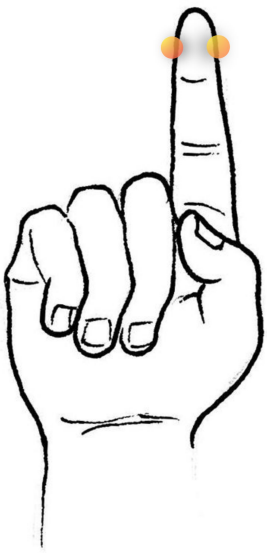

FIGURE 6.1: Location of Vibration Stimulation [Ada19]

Based on these guidelines, the two points of stimulation on the fingertip are proposed (see Figure 6.1) based on the following reasons:

- The device developed should hinder the underside of the fingertip consisting of the epidermal ridges as little as possible. This enables the user to interact with real objects without removing the device.
- The stimulation points should be close to the fingerprint region, which is one of the most sensitive areas of the human body.
- The stimulation points must be far apart from each other, so that the receptive fields do not overlap with each other. This enables localised vibration from both the actuators which can be perceived independently, resulting in higher degrees of information to the user.

6.2 3D Printing

3D Printing, also called additive manufacturing, includes the design of the object in a CAD environment and then, manufacturing it with a 3D printer. Makerbot Replicator 2 printer from Makerbot Industries (Figure 6.2b) was used for developing the prototype, which works on the principle of Fused Deposition Modeling (FDM). In

FDM process, the product is built layer-by-layer after the 3D model is converted into a G-Code; code in which the model has been mathematically sliced and coordinated. It is an effective method to fabricate a working prototype in terms of cost and time consumption. Figure 6.2a shows the basic idea of FDM printing process.

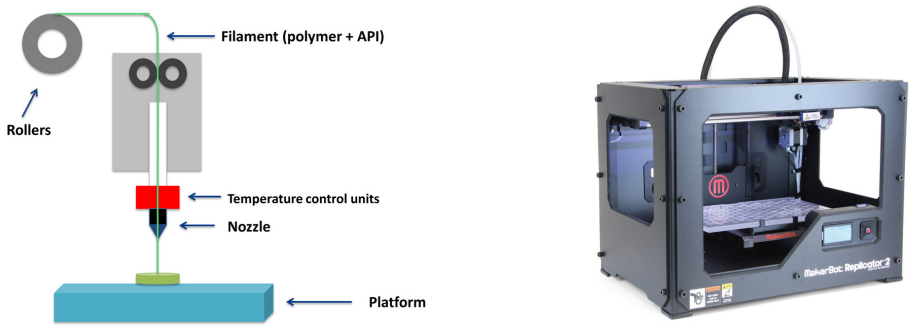

(A) FDM printing process. [KGPS17] (B) Makerbot Replicator 2. [Mak19]

FIGURE 6.2: 3D Printing

One of the most important aspects in 3D printing is to select the material that is used, which has a big impact on the final product. The materials have different properties that are chosen to meet our needs. The important factors for better user's acceptance and experience of a wearable device is comfort and adaptability, as discussed in Chapter 4. Adaptability refers to the possibility of the device to fit different shape/size of a finger. Comfort involves acceptance of texture and weight, enabling users to have natural movements while performing the tasks without any constraints. Thermoplastics are very well suited for functional applications because they have good mechanical properties and high impact resistance [SD19]. Thermoplastics such as ABS and Nylon are also widely used with injection molding process to produce wearable devices in mass production. In order to fit different finger sizes and achieve a proper fit, a flexible thermoplastic material was used which permits the device to be flexed under load.

Polypropylene (PP) is a flexible 3D-print material that can be flexed easily as they it is elastic in nature. It has advantages over standard 3D printing filaments like PLA, with good flexibility and lightweight characteristics. PP also has better resistance to deformation under load, which qualifies it to fit different finger sizes that assume additional bending. It has the lowest density among commonly used

materials and good strength to weight ratio, to withstand higher loads. Due to its semi-crystalline nature of PP, it solidifies differently after cooling resulting in warping. So it is important to have the right Slicer settings to ensure a good print quality [YTL+17].

Slicer Settings

Slicer is a 3D printing software that takes CAD model as the input and cuts it onto 3D printing layers. Then, all the information is bundled up in a G-Code which is sent to the printer. Simplify3D software was used to customize the 3D printer settings. The recommended bed and extruder temperatures to print PP are 90°C and 220-240°C. Some of the other settings which are important for a good print quality are:

Extruder Settings

Most of the problems that occur during a 3D printing process is during the filament extrusion. Therefore, some of the adjustments made to the extruder settings (see Figure 6.3) are:

- Extrusion multiplier: This controls the rate of flow of material from the extruder. The value of extrusion multiplier was set to 1 (100%).
- Retraction distance: As the extrusion temperature of PP is higher than materials like PLA or ABS, it is important to determine how much filament is pulled out when nozzle is retracted. Therefore, the retraction distance was increased to 6mm to avoid oozing of the filament from the nozzle.
- Coasting distance: High print temperature of PP may result in overextrusion, which means that some extra filament is extruded. The coasting distance will help to compensate some of this extra material to avoid defects.

Layer Settings

The FDM printing process builds a part layer-by-layer, due to which the thickness of each layer will determine the resolution of a print. PP is prone to warping due to

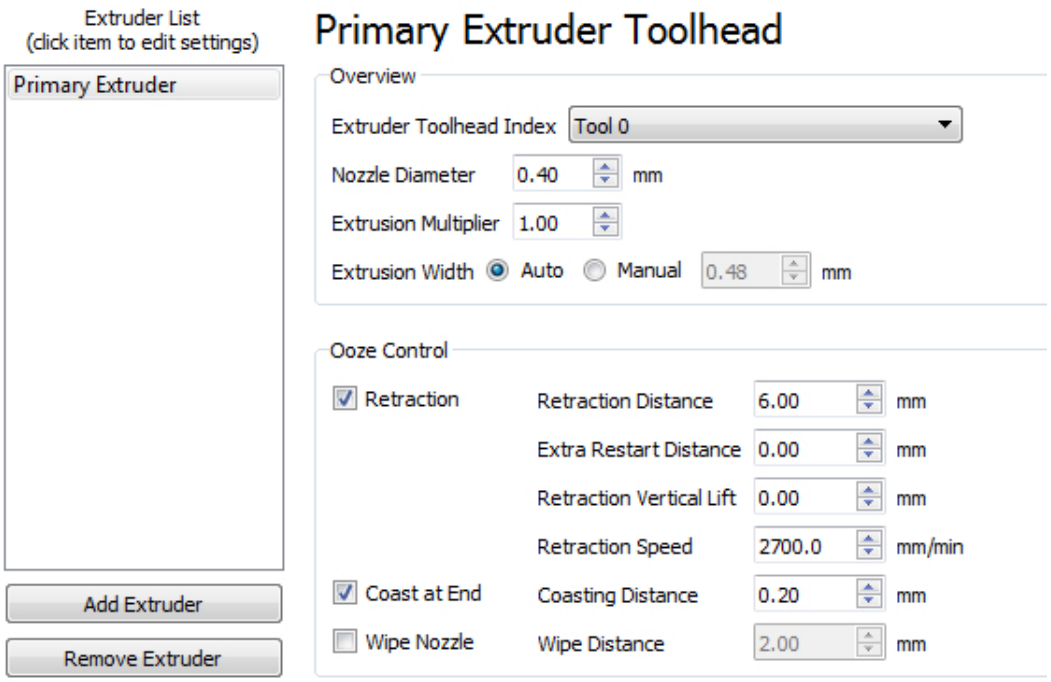

FIGURE 6.3: Extruder Settings for PP in Simplify3D Software

material shrinkage, and this causes the corners to lift up from the build plate. One of the ways to avoid warping is to have a heated build plate set to the temperature just above the point where the material solidifies. This helps the material to be connected to the build plate without solidifying. Another way to make sure that the material sticks to the build plate is by controlling the first layer speed. With low initial layer speeds, the material has enough time to adhere to the plate.

6.3 Mechanical Structure

A mechanical structure was designed and developed for a modular tactile device based on the design guidelines. The prototype was designed to fit on the distal phalanges of the index finger, specifically for the user to be able to touch real objects without any hindrance and also, to interact with objects in VE by means of vibrational feedback. The device consists mainly of three parts: the main body, actuators and the lever arms to position the actuators. By taking advantage of rapid prototyping, it was possible to design and print several different iterations to ensure a functional prototype at the end. Some of the early prototypes were designed to test the

right fit on the fingertip and the placement of the two actuators. These designs can be found in Appendix B. When the actuators are directly placed on the main body, the vibrations are transmitted through the entire structure and the stimulation's are not localized. After the assessment of the initial prototypes, a functional prototype of the tactile display was developed (see Figure. 6.4). In this prototype, the actuators are located on either side of the main body to provide stimulation using lever arms.

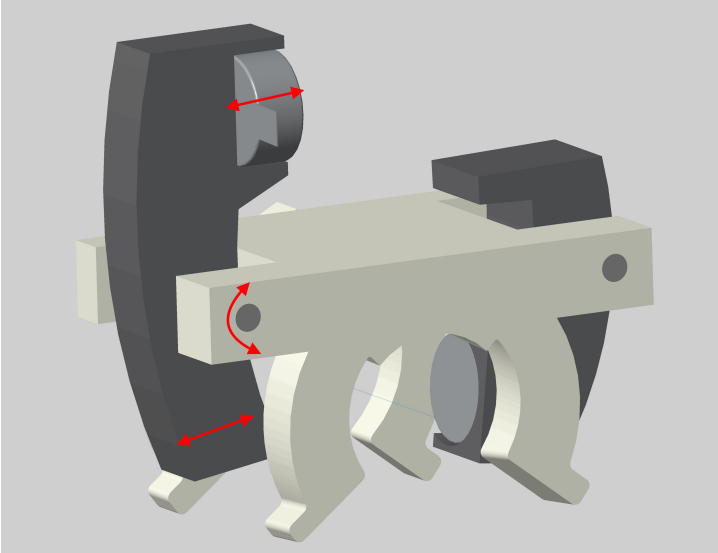

FIGURE 6.4: CAD model of the Functional Prototype

The device uses two different methods for tactile stimulation on either side. On one side of the device, the vibrations from the actuator transmits high-frequency repeated stimulation through the lever arms. As the actuator vibrates along the longitudinal axis, the motion is transmitted through the hinge to the contact area on the lower side of the device. On the other side, the actuator is positioned on the lower side such that, it is in direct contact with the skin to provide stimulation. The lever arms are mainly used for two reasons.

- First, if the actuators are in direct contact with the main body, the vibrations are transmitted throughout the fingertip and localised vibrations cannot be perceived.
- Second, the device dimension is minimized on the bottom and the sides of the finger as the actuators are placed on the top side of the device (i.e., on the

fingernail side). Due to this, there is also freedom of movement, and space between the device and the adjacent finger.

The main body and the lever arms are printed using the 3D printer. As discussed in Section 6.2, a flexible material was used to print the main body to accommodate different finger sizes. The inner radius of the body which clamps onto the finger, is based on the average width of the index finger for a human, i.e., 16 - 20 mm in most adults [DRS03]. As the lever arms are small in size and require high resolution 3D prints, it was difficult to print with the flexible material. Hence, PLA was used to print the lever arms, which has good strength and durability. It is also very easy to print small parts with PLA.

6.4 Chapter Summary

In this Chapter, the mechanical construction of the fingertip device based on different functionality requirements was presented. As two actuators are used on the device, the points of stimulation are first investigated. The requirement of a flexible filament to print the main structure of the device was also discussed.

The functional prototype was developed with a hinge mechanism to transmit the vibration via the lever arms. In the next chapter, the two different methods implemented for tactile stimulation to determine the optimal design in terms of placement of the actuators are compared and evaluated. Any reduction in tactile stimulus due to the transmission of vibration via a lever arm is also investigated.

Chapter 7

Evaluation Study

In Chapter 6, we presented two different methods for tactile stimulation on either side of the device. It is now important to evaluate them based on the functional requirements of the device. In this Chapter, we discuss the evaluation tests conducted to investigate the placement of the two actuators. The evaluation study is divided into two sections. First, we measure the maximum force that is applied on the stimulation points by these two methods. Second, a subjective evaluation with a small group of participants to compare the intensity and localization between the two methods is analyzed.

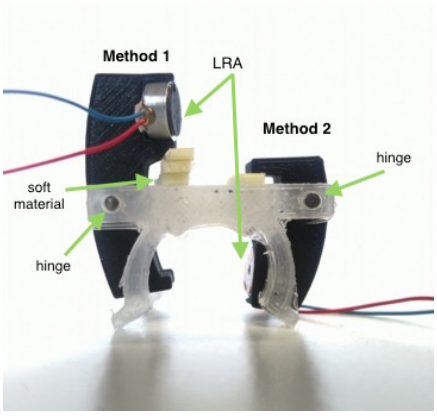

(A) Functional Prototype of the tactile device to compare the two methods of actuation

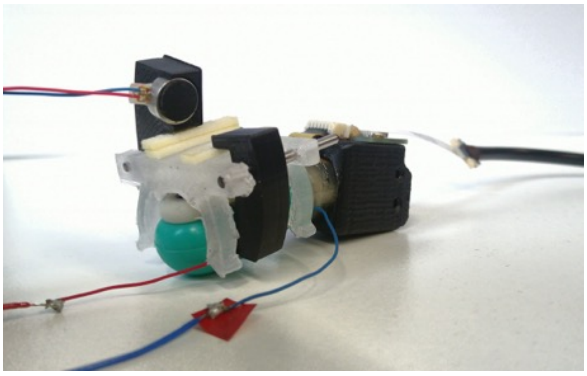

(B) Prototype on a BioTac sensor to measure the force applied

FIGURE 7.1: Haptic Thimble Prototype

To simplify for better understanding, we use the terminologies Method 1 and Method 2. 'Method 1' is the transmission of vibration through the lever arm, in which the actuator is positioned on the upper side (fingernail side) of the device.

'Method 2' is the stimulation due to direct contact of the skin with the actuator positioned on the lower side of the device (fingerprint side) (see Figure 7.1a).

7.1 Technical Evaluation

The maximum force applied by the two methods was measured using a BioTac tactile sensor by SynTouch Inc.(see Figure 7.1b). The BioTac consists of three different sensors to detect temperature, contact and surface properties of the touched object. Figure 7.2 shows the sideways cross-section with the technical structure of BioTac sensor. The first sensor is a hydro-acoustic pressure sensor that measures the pressure of the incompressible conductive field inside the flexible silicone skin. Microvibrations are also measured by providing a high-pass filter version of this data. The thermistor is the second sensor used to measure the temperature, which is also high-pass filtered to provide thermal flux. The third sensor is a set of 19 electrodes, which are placed on different locations of the BioTac's surface to detect impedance changes. [FLL13]

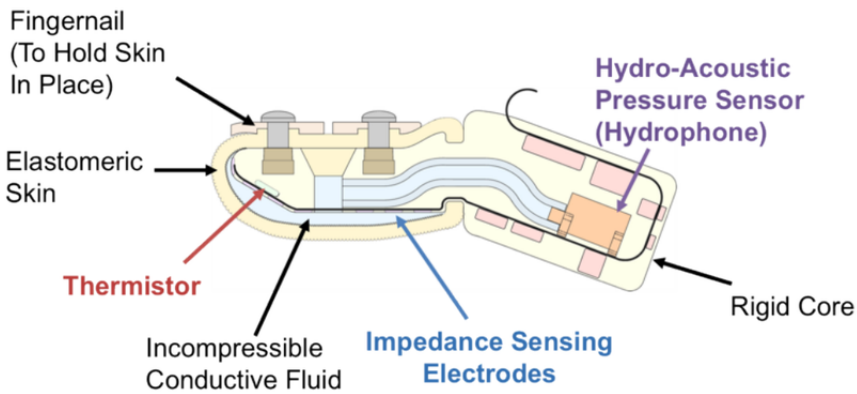

FIGURE 7.2: A schematic diagram of a BioTac biomimetic tactile sensor. Source: [SFYL12]

The microprocessor inside the BioTac samples and digitize all the values from the sensors at 12 bits. The communication between the BioTac and PC is done using Serial Peripheral Interface (SPI) interface. The responses from the sensors are read individually by the host and displayed on the BioTac GUI Software.

To measure the force of actuation produced by the two methods, the Arduino interface implemented earlier in Chapter 5 was instructed to send similar PWM signal to both the actuators. The magnitude of forces from both the methods displayed in the BioTac software are as shown in Figure 7.3

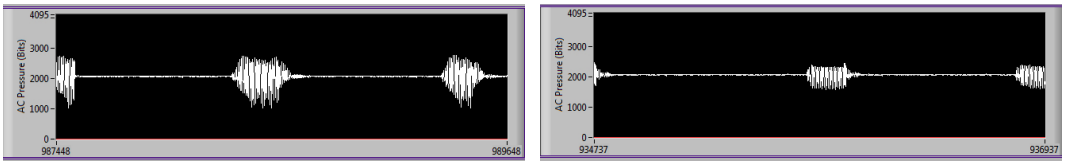

(A) Magnitude of force by Method 1 (B) Magnitude of force by Method 2

FIGURE 7.3: Force Measurement using BioTac sensor and its software

The DC Pressure (Pdc) or static pressure read from the sensor represents both the normal and shear force. The Pdc value increases linearly with the fluid pressure. As seen in Figure 7.2, it has both high and low values due to distortion of the fluid in both directions when a force is applied. It can also be observed that the fluid distortion or range of Pdc is higher in Method 1 than in Method 2, which implies that the force of vibration transmitted through the lever arm is greater than the force of vibration due to direct contact of the skin with the actuator. In other words, Method 1 is more effective in terms of force and intensity when compared to Method 2.

Pressure is defined as force over area. So, when the force is applied on a smaller area in Method 1, the impact on the skin feels an increased applied force. This is simply because it has less area to dissipate the same amount of force. In Method 2, the force is applied over a larger surface area when the actuator is in direct contact with the skin. Therefore, using Method 1 as the primary way for tactile stimulus will provide better localized vibration and higher vibrational force.

7.2 Subjective Evaluation

The objective of this subjective evaluation was to evaluate the ergonomics of the prototype device and also compare the placement of the actuators based on:

- the intensity of vibration, which is directly related to the force applied on the skin.
- the localization of vibration.

Methods

Task: The task was to compare the intensity and localisation of vibration between the two actuation methods. The participant wears the device on the index finger in both the conditions and the actuators on both the sides stimulate with different vibration patterns. During the experiment, the user was not previously informed about which actuator will be actuated before starting the actuator. This helped us evaluate the study without any bias. The experiment was also performed by fitting the device in the other direction, where the positions of the actuation methods are reversed. This was done due to the fact that, some participants may have higher sensitivity on one of their fingertip than the other. By reversing the device and repeating the experiment, this will be negated to a great extent to evaluate the two methods accurately.

Participants: Nine right-handed participants and one left-handed participant of the DLR community took part in this study. Four of these participants had previous experiences with haptic feedback systems.

Metrics: For each condition, we recorded the participant's score on the scale of 1 to 7. Then, we measured the user's sense of discomfort and other aspects of performance using the NASA Test Load Index (NASA-TLX) assessment tool [Har06] . (See questionnaire in Appendix C)

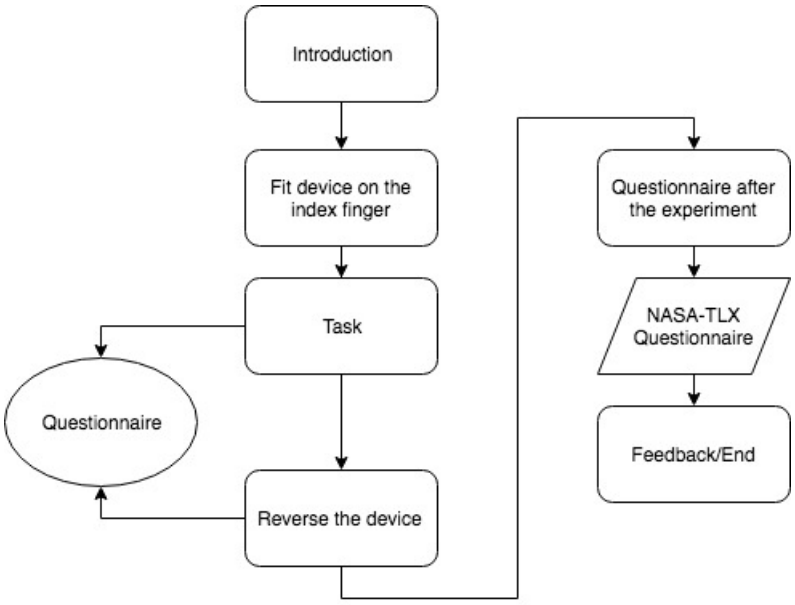

FIGURE 7.4: An overview of the user evaluation procedure

Procedure: We first introduce the participant to the purpose of evaluation and provide the outline of this thesis. Second, we present an overview for the tasks and explain how the participants has to score for each condition. As mentioned previously, the tasks were not explained in detail initially so that the scores are unbiased. Third, we fit the device on the index finger of the participant and ensure it is comfortable. Fourth, we start the experiment by giving input to the actuators in different patterns, during which the participant was asked to provide the scores. Fifth, we ask the participant to repeat the same conditions after changing the direction of the device. After the experiments, the participant was asked score the device based on fatigue and comfort. Lastly, we ask the participant to fill out the Performance Assessment Questionnaire while still wearing the device. An overview of the procedure is shown in Figure 7.4.

Result

The total number of questions completed by all the participants were 140 questions (10 participants x 7 questions x 2 change the direction). It took about 20 minutes for each participant to complete their entire evaluation.

Experiment: An experiment was conducted to compare the two methods of actuation based on localization and intensity of vibration perceived on the fingers. There was a significant difference in the scores for both the methods. The following three questions yielded the most important results:

- Q1. How easy was it to perceive the location of vibration?
- Q2. How is the intensity of feedback?
- Q3. Did the device cause any fatigue due to weight?
- Q4. Did the device cause any discomfort due to vibrations?
- Q5. Which method provides better vibration localization?

The participants were asked to rate these questions on a Likert scale of one to seven. The users clearly had a better feedback experience from Method 1, due to good intensity (M=4.7, SD=0.9) and better localized vibration (M=4.75, SD=1.7) as seen in Figure 7.5a. The fatigue caused by the overall device has very low scores (M=1.6, SD=0.6), verifying that the device was well received in this regard . Also, in terms of better localization of vibration on a different y-axis scale (see Figure 7.5b), Method 1 has a better score when compared to Method 2 (M=4.8, SD=1.67). Table 7.1 summarizes the results of the NASA-TLX questionnaire for 10 participants. These studies confirm the suitability of the concept and clearly underline its potential for the use as wearable haptic device in various mobile haptic applications, in particular for augmented haptic feedback.

TABLE 7.1: Nasa-TLX workload scores. min value=1, max value=20

Dimensions	Mean	Standard Deviation
Mental Demand	4.5	2.34
Physical Demand	4	2.4
Temporal Demand	2	1.33
Effort	2.5	2.92
Frustration	1.5	1.28

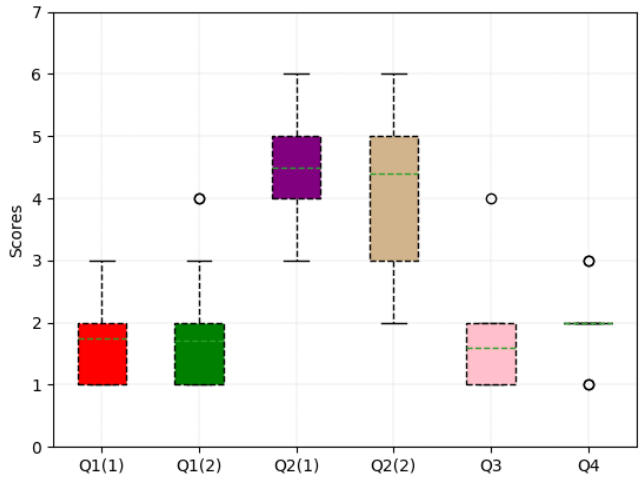

(A) Result for intensity and fatigue. Q1 (1)and Q2(1) are scores for Method 1. Q1 (2)and Q2 (2) are scores for Method 2.

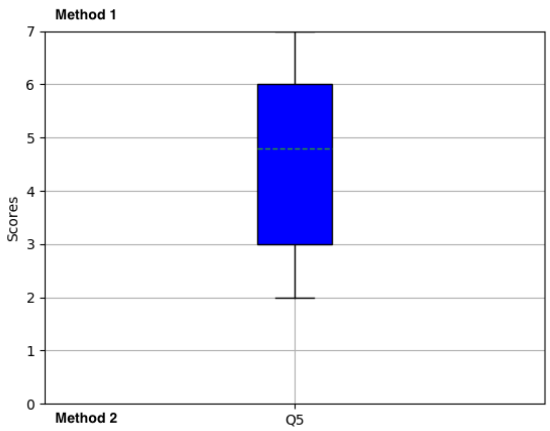

(B) Score to compare the localization of vibration of the two Methods. The scale on the y-axis goes from Method 2 to Method 1 as it increases.

FIGURE 7.5: Result to compare the localization of two Methods

These studies confirm the suitability of the concept and clearly underline its potential for the use as wearable haptic device in various mobile haptic applications, in particular for augmented haptic feedback.

Chapter 8

Conclusion

In order to develop a functioning prototype of a fingertip tactile device, an exhaustive study was conducted. Existing haptic devices were investigated and the various tactile technologies were studied. The devices were found to be bulky and did not provide support for interacting with both virtual and real objects simultaneously. To achieve compactness, various actuation technologies were compared and linear resonant actuators were found to be a good candidate. Also, power efficiency of LRAs were better compared to the other actuators.

After choosing the actuator, to develop the tactile device, four design guidelines were followed. They were weight, comfort, form factor and impairment. ESP32 microcontroller was chosen due to its compactness, low cost and low power consumption. Time-of-Flight (Adafruit VL6180x ToF sensor) sensor was also used to measure the distance to the real objects when working in augmented reality. The LRA used in our prototype is ELV1036, which is a y-axis linear vibrator and vibrates perpendicular to the mounting plane. The frequency range of this particular LRA is 205 ± 5 Hz, which lies within the bandwidth of the frequency of the skin. To drive this LRA, motor driver DRV2605 from Texas Instruments was chosen. The main advantages of this driver are precise vibrations due to active braking and smart-loop characteristics. It also uses I2C communication lines which helps with easier integration with the microcontroller.

The functions for ToF interface and motor driver interface were developed using C++ language. The functions developed for the ToF interface were used to measure the distance of the real objects and that developed for the motor driver interface were

to drive the LRAs at the resonant frequency and the required vibration patterns. These two interfaces were later integrated with the microcontroller using Arduino program.

To achieve higher degrees of freedom of sense of touch and increase accuracy, two LRAs were used on either side of the fingertip. Optimum location for placement of LRAs was decided based on various criteria. For the functional prototype, different 3D printing materials were considered. Polypropylene was chosen due to its higher strength to weight ratio and flexibility.

The functional prototype was developed with two different methods of tactile actuations. First method was the transmission of vibration through lever arm and the second method was tactile stimulation due to direct contact of the skin with the LRA. Both technical and user evaluation studies were conducted on the two methods. In the technical evaluation, a BioTac sensor was used to measure the pressure at the contact points of the LRAs. It was observed that better vibrational force and localized vibration was found in the first method. For the user evaluation, 10 participants were asked to describe the localization and intensity of vibration from the two methods. The participants were asked to rate these questions on a Likert scale of one to seven. The users clearly had a better feedback experience from Method 1, due to good intensity and better localized vibration. In addition, the users did not feel any discomfort or fatigue upon wearing the device on the fingertips. This was due to the lower weight and better fit of the tactile device, which was one of the important design criteria. Both these studies proved that method which uses the lever arm to transmit the vibration yielded the best results.

The overall results indicate that that functioning device is a promising start to interact simultaneously with virtual and real objects. On the whole, the proposed device is a cost effective and lightweight device, with two actuators that can produce enough force on the skin to sense different tactile modalities.

8.1 Future Work

This thesis introduced a functional demonstrator during the initial concept phase. There are some of the aspects which were not included in this initial prototype and can be delegated as future work. One of these aspects is the integration of a 3D virtual environment. A simulation with common test scenarios can be developed, which can be coupled with the hardware. The device can also include a motion tracking system to engage and interact with the virtual world.

Further changes in the hardware setup such as, reducing the wiring and designing a new PCB without the breakout boards can make the system more compact and easy to integrate. It will also result in ease of movement and reduce the weight even further. It is also possible to implement wireless communication between the components, as the ESP32 already has wireless capabilities.

Despite the positive results, future research can be done to investigate the use of alternate forms of tactile feedback. The viability of alternate forms of input, such as pressure, stretch and heat, will certainly add more layers of information between the user and the virtual objects, providing a more immersive level of interaction. Adding additional forms of tactile feedback may also be beneficial to users undergoing medical training.

All things considered, an interesting design was proposed for tactile devices that can be used not just in VEs, but also in AEs. In combination with provided enhancements and refinements, this will provide an opportunity to increase the usability of haptic devices and enhance the user experience. We are curious about the progress in the field of tactile feedback and looking forward for better implementations of this technology in the near future.

Bibliography

[Ada19] Adafruit. *DRV2605 Datasheet*, Accessed: November 17, 2019. Online.

[ASM94] Motoyuki Akamatsu, Sigeru Sato, and I Scott MacKenzie. Multimodal mouse: A mouse-type device with tactile and force display. *Presence: Teleoperators & Virtual Environments*, 3(1):73–80, 1994.

[BAG92] Bryan Buchholz, Thomas J Armstrong, and Steven A Goldstein. Anthropometric data for describing the kinematics of the human hand. *Ergonomics*, 35(3):261–273, 1992.

[BB96] Grigore C Burdea and Frederick P Brooks. Force and touch feedback for virtual reality. 1996.

[BC09] Yoseph Bar-Cohen. Electroactive polymers for refreshable braille displays. *SPIE Newsroom*, 11, 2009.

[BCZ+99] Ray H Baughman, Changxing Cui, Anvar A Zakhidov, Zafar Iqbal, Joseph N Barisci, Geoff M Spinks, Gordon G Wallace, Alberto Mazzoldi, Danilo De Rossi, Andrew G Rinzler, et al. Carbon nanotube actuators. *Science*, 284(5418):1340–1344, 1999.

[BMS03] Stephen Brewster and Roderick Murray-Smith. *Haptic Human-Computer Interaction: First International Workshop, Glasgow, UK, August 31-September 1, 2000, Proceedings*, volume 2058. Springer, 2003.

[BN99] Ion Boldea and Syed A Nasar. Linear electric actuators and generators. *IEEE Transactions on Energy Conversion*, 14(3):712–717, 1999.

[Bur96] GC Burder. Force and touch feedback for virtual reality. *A Wiley-Interscience Publication*, pages 13–40, 1996.

[Bur00] Grigore C Burdea. Haptics issues in virtual environments. In *Proceedings Computer Graphics International 2000*, pages 295–302. IEEE, 2000.

[CK12] Seungmoon Choi and Katherine J Kuchenbecker. Vibrotactile display: Perception, technology, and applications. *Proceedings of the IEEE*, 101(9):2093–2104, 2012.

[CMPP15] Francesco Chinello, Monica Malvezzi, Claudio Pacchierotti, and Domenico Prattichizzo. Design and development of a 3rrs wearable fingertip cutaneous device. In *2015 IEEE International Conference on Advanced Intelligent Mechatronics (AIM)*, pages 293–298. IEEE, 2015.

[CSO18] Heather Culbertson, Samuel B Schorr, and Allison M Okamura. Haptics: The present and future of artificial touch sensation. *Annual Review of Control, Robotics, and Autonomous Systems*, 1:385–409, 2018.

[CTC+11] CJ Camargo, N Torras, H Campanella, JE Comrie, EM Campo, K Zinoviev, EM Terentjev, and J Esteve. Light-actuated cnt-doped elastomer blisters towards braille dots. In *2011 16th International Solid-State Sensors, Actuators and Microsystems Conference*, pages 1594–1597. IEEE, 2011.

[DCMD00] Jonathan Downar, Adrian P Crawley, David J Mikulis, and Karen D Davis. A multimodal cortical network for the detection of changes in the sensory environment. *Nature neuroscience*, 3(3):277, 2000.

[DRS03] Kiran Dandekar, Balasundar I Raju, and Mandayam A Srinivasan. 3-d finite-element models of human and monkey fingertips to investigate the mechanics of tactile sense. *Journal of biomechanical engineering*, 125(5):682–691, 2003.

[Esp19a] Espressif. *ESP32 Datasheet*, Accessed: November 09, 2019. https://www.espressif.com/sites/default/files/documentation/0a-esp8266ex_datasheet_en.pdf.

[Esp19b] Espressif. *ESP8266EX Datasheet*, Accessed: September 30, 2019. https://www.espressif.com/sites/default/files/documentation/0a-esp8266ex_datasheet_en.pdf.

[Fie98] Tiffany M Field. Touch therapy effects on development. *International Journal of Behavioral Development*, 22(4):779–797, 1998.

[FLL13] Jeremy Fishel, Gary Lin, and GE Loeb. Biotac product manual. 2013.

[Gib66] James Jerome Gibson. The senses considered as perceptual systems. 1966.

[GKS+98] F. Gemperle, C. Kasabach, J. Stivoric, M. Bauer, and R. Martin. Design for wearability. In *Proceedings of the 2Nd IEEE International Symposium on Wearable Computers*, ISWC '98, pages 116–, Washington, DC, USA, 1998. IEEE Computer Society.

[GWV09] GA Gescheider, JH Wright, and RT Verrillo. Information-processing channels in the tactile sensory system: A psychophysical and physiological analysis new york, 2009.

[GWV10] George A Gescheider, John H Wright, and Ronald T Verrillo. *Information-processing channels in the tactile sensory system: A psychophysical and physiological analysis*. Psychology press, 2010.

[HACH+04] Vincent Hayward, Oliver R Astley, Manuel Cruz-Hernandez, Danny Grant, and Gabriel Robles-De-La-Torre. Haptic interfaces and devices. *Sensor review*, 2004.

[Har06] Sandra G Hart. Nasa-task load index (nasa-tlx. In *Proceedings of the human factors and ergonomics society annual meeting*, volume 50, pages 904–908. Sage publications Sage CA: Los Angeles, CA, 2006.

[HDCD11] Arindam Halder, Ranjan Dasgupta, Jayakar Chepada, and Nrusingh Prasad Dash. Implementation of mcu invariant i2c slave driver using bit banging. 2011.

[IEVO09] Ali Israr, Dillon P Eng, Sastry S Vedam, and Marcia K O'Malley. A low cost vibrotactile array to manage respiratory motion. In *World Haptics 2009-Third Joint EuroHaptics conference and Symposium on Haptic Interfaces for Virtual Environment and Teleoperator Systems*, pages 619–620. IEEE, 2009.

[IKB+03] Tanya Imai, Sandra Kamping, Caterina Breitenstein, Christo Pantev, Bernd Lütkenhöner, and Stefan Knecht. Learning of tactile frequency discrimination in humans. *Human brain mapping*, 18(4):260–271, 2003.

[Jar83] Ray A Jarvis. A laser time-of-flight range scanner for robotic vision. *IEEE Transactions on Pattern Analysis and Machine Intelligence*, (5):505–512, 1983.

[JS08] Lynette A Jones and Nadine B Sarter. Tactile displays: Guidance for their design and application. *Human factors*, 50(1):90–111, 2008.

[JSZM15] Lina Jia, Zhuanghua Shi, Xuelian Zang, and Hermann J Müller. Watching a real moving object expands tactile duration: the role of task-irrelevant action context for subjective time. *Attention, Perception, & Psychophysics*, 77(8):2768–2780, 2015.

[Ker08] Thorsten A Kern. *Entwicklung Haptischer Geräte: Ein Einstieg für Ingenieure (German); Development of Haptic Devices: An Introduction to Engineers*. Springer, 2008.

[KGPS17] Andrea Alice Konta, Marta García-Piña, and Dolores R Serrano. Personalised 3d printed medicines: which techniques and polymers are more successful? *Bioengineering*, 4(4):79, 2017.

[KKT02] Hiroyuki Kajimoto, Naoki Kawakami, and Susumu Tachi. Optimal design method for selective nerve stimulation and its application to electrocutaneous display. In *Proceedings 10th Symposium on Haptic Interfaces for Virtual Environment and Teleoperator Systems. HAPTICS 2002*, pages 303–310. IEEE, 2002.

[KRI06] Timo Kahlmann, Fabio Remondino, and Hilmar Ingensand. Calibration for increased accuracy of the range imaging camera swissrangertm. *Image Engineering and Vision Metrology (IEVM)*, 36(3):136–141, 2006.

[KWByRT91] Kurt A Kaczmarek, John G Webster, Paul Bach-y Rita, and Willis J Tompkins. Electrotactile and vibrotactile displays for sensory substitution systems. *IEEE Transactions on Biomedical Engineering*, 38(1):1–16, 1991.

[LLC19] CyberForce CyberGlove Systems LLC. Accessed October 3, 2019. http://www.cyberglovesystems.com/cyberforce.

[LLDA+12] Márcio D Lima, Na Li, Monica Jung De Andrade, Shaoli Fang, Jiyoung Oh, Geoffrey M Spinks, Mikhail E Kozlov, Carter S Haines, Dongseok Suh, Javad Foroughi, et al. Electrically, chemically, and photonically powered torsional and tensile actuation of hybrid carbon nanotube yarn muscles. *Science*, 338(6109):928–932, 2012.

[LN99] Mark H Lee and Howard R Nicholls. Review article tactile sensing for mechatronics—a state of the art survey. *Mechatronics*, 9(1):1–31, 1999.

[LZZ+12] Shan Li, Xiaohua Zhang, Jingna Zhao, Fancheng Meng, Geng Xu, Zhenzhong Yong, Jingjing Jia, Zuoguang Zhang, and Qingwen Li. Enhancement of carbon nanotube fibres using different solvents and polymers. *Composites science and technology*, 72(12):1402–1407, 2012.

[MAB+19] C Mehring, M Akselrod, L Bashford, M Mace, H Choi, M Blüher, A-S Buschhoff, T Pistohl, R Salomon, A Cheah, et al. Augmented manipulation ability in humans with six-fingered hands. *Nature communications*, 10(1):2401, 2019.

[Mak19] MakerBot. *MakerBot Replicator 2*, Accessed: October 30, 2019. Online.

[Mao14] N Mao. Towards objective discrimination & evaluation of fabric tactile properties: Quantification of biaxial fabric deformations by using energy methods. In *Leeds Proceedings*, 2014.

[MEBA15] Nader A Mansour, Ahmed MR Fath El-Bab, and Samy FM Assal. A novel sma-based micro tactile display device for elasticity range of human soft tissues: Design and simulation. In *2015 IEEE International Conference on Advanced Intelligent Mechatronics (AIM)*, pages 447–452. IEEE, 2015.

[Mic19a] Precision Microdrives. *AB-004 : Understanding ERM Vibration Motor Characteristics*, Accessed: October 12, 2019. Online.

[Mic19b] Precision Microdrives. *AB-020 : Understanding Linear Resonant Actuator Characteristics*, Accessed: October 12, 2019. Online.

[MMT+05] Tsuneo Matsunaga, W Makishi, K Totsu, M Esashi, and Y Haga. 2-d and 3-d tactile pin display using sma micro-coil actuator and magnetic latch. In *The 13th International Conference on Solid-State Sensors, Actuators and Microsystems, 2005. Digest of Technical Papers. TRANSDUCERS'05.*, volume 1, pages 325–328. IEEE, 2005.

[MPC+17] Maurizio Maisto, Claudio Pacchierotti, Francesco Chinello, Gionata Salvietti, Alessandro De Luca, and Domenico Prattichizzo. Evaluation of wearable haptic systems for the fingers in augmented reality applications. *IEEE transactions on haptics*, 10(4):511–522, 2017.

[MPT05] William A McNeely, Kevin D Puterbaugh, and James J Troy. Six degree-of-freedom haptic rendering using voxel sampling. In *ACM SIGGRAPH 2005 Courses*, page 42. ACM, 2005.

[MS+94] Thomas H Massie, J Kenneth Salisbury, et al. The phantom haptic interface: A device for probing virtual objects. In *Proceedings of the ASME winter annual meeting, symposium on haptic interfaces for virtual environment and teleoperator systems*, volume 55, pages 295–300. Citeseer, 1994.

[MT19] Inc. Mimic Technologies. *Da Vinci Trainer*, Accessed: October 11, 2019.

[MUNM19] Suvrajyoti Mishra, Lakshmi Unnikrishnan, Sanjay Kumar Nayak, and Smita Mohanty. Advances in piezoelectric polymer composites for energy harvesting applications: a systematic review. *Macromolecular Materials and Engineering*, 304(1):1800463, 2019.

[NFPMC19] Ltd Need For Power Motor CO. *Linear Resonant Actuators: ELV1036*, Accessed: November 24, 2019. Online.

[NTM+01] Takaaki Nara, Masaya Takasaki, Taro Maeda, Toshiro Higuchi, Shigeru Ando, and Susumu Tachi. Surface acoustic wave (saw) tactile display based on properties of mechanoreceptors. In *Proceedings IEEE Virtual Reality 2001*, pages 13–20. IEEE, 2001.

[PCH+11] Gunhyuk Park, Seungmoon Choi, Kyunghun Hwang, Sunwook Kim, Jaecheon Sa, and Moonchae Joung. Tactile effect design and evaluation for virtual buttons on a mobile device touchscreen. In *Proceedings of the 13th International Conference on Human Computer Interaction with Mobile Devices and Services*, pages 11–20. ACM, 2011.

[PPK15] Claudio Pacchierotti, Domenico Prattichizzo, and Katherine J Kuchenbecker. Displaying sensed tactile cues with a fingertip haptic device. *IEEE transactions on haptics*, 8(4):384–396, 2015.

[PSH+16] Claudio Pacchierotti, Gionata Salvietti, Irfan Hussain, Leonardo Meli, and Domenico Prattichizzo. The hring: A wearable haptic device to avoid occlusions in hand tracking. In *2016 IEEE Haptics Symposium (HAPTICS)*, pages 134–139. IEEE, 2016.

[SD19] Inc. Stratasys Direct. *Key Considerations when 3D Printing with Thermoplastics*, Accessed: November 22, 2019.

[SFRS04] Salvador Soto-Faraco, Angelica Ronald, and Charles Spence. Tactile selective attention and body posture: assessing the multisensory contributions of vision and proprioception. *Perception & Psychophysics*, 66(7):1077–1094, 2004.

[SFYL12] Zhe Su, Jeremy A Fishel, Tomonori Yamamoto, and Gerald E Loeb. Use of tactile feedback to control exploratory movements to characterize object compliance. *Frontiers in neurorobotics*, 6:7, 2012.

[Ske12] Lisa Skedung. *Tactile perception: role of friction and texture*. PhD thesis, KTH Royal Institute of Technology, 2012.

[SSCR01] Lazar Stankov, Tatjana Seizova-Cajić, and Richard D Roberts. Tactile and kinesthetic perceptual processes within the taxonomy of human cognitive abilities. *Intelligence*, 29(1):1–29, 2001.

[ST70] Robert M Strong and Donald E Troxel. An electrotactile display. *IEEE Transactions on Man-Machine Systems*, 11(1):72–79, 1970.

[STM19a] STMicroelectronics. *VL6180X Datasheer*, Accessed: November 24, 2019. Online.

[STM19b] STMicroelectronics. *VL6180X Datasheet*, Accessed: October 15, 2019. https://www.st.com/resource/en/datasheet/vl6180x.pdf.

[TKMN04] Masaya Takasaki, Hiroyuki Kotani, Takeshi Mizuno, and Takaaki Nara. Reproduction of tactile sensation using saw tactile display. In *IEEE Conference on Robotics and Automation, 2004. TExCRA Technical Exhibition Based.*, pages 67–68. IEEE, 2004.

[Ver66] Ronald T Verrillo. Vibrotactile thresholds for hairy skin. *Journal of Experimental Psychology*, 72(1):47, 1966.

[XLY+17] Xin Xie, Sanwei Liu, Chenye Yang, Zhengyu Yang, Tian Liu, Juncai Xu, Cheng Zhang, and Xianglin Zhai. A review of smart materials in tactile actuators for information delivery. *C—Journal of Carbon Research*, 3(4):38, 2017.

[YCHH04] Akio Yamamoto, Benjamin Cros, Hironori Hashimoto, and Toshiro Higuchi. Control of thermal tactile display based on prediction of contact temperature. In *IEEE International Conference on Robotics and Automation, 2004. Proceedings. ICRA'04. 2004*, volume 2, pages 1536–1541. IEEE, 2004.

[YTL+17] Chuncheng Yang, Xiaoyong Tian, Dichen Li, Yi Cao, Feng Zhao, and Changquan Shi. Influence of thermal processing conditions in 3d printing on the crystallinity and mechanical properties of peek material. *Journal of Materials Processing Technology*, 248:1–7, 2017.

[ZKK+04] Rui Zhang, Andreas Kunz, Gabor Kovac, Silvain Michel, and Andrea Mazzone. Dielectric elastomer actuators for a portable force feedback device. In *Proceedings: proceedings of the 4th International Conference EuroHaptics 2004*, pages 300–307. Institute of Automatic Control Engineering (LSR), Technische Universität München, 2004.

[ZP12] Vladimir M Zatsiorsky and Boris I Prilutsky. *Biomechanics of skeletal muscles*. Human Kinetics, 2012.

Appendix A

Arduino Code

A.1 TOF sensor

```
#include "Arduino.h"
#include <Wire.h>

#define I2C_ADDR 0x29  ///< The fixed I2C address

// Interrupt configuration
#define INTERRUPT_CLEAR         0x015
// Fresh out of reset bit
#define SYSTEM_RESET            0x016
/ Trigger Ranging
#define RANGE_START             0x0181
// Range Status for errors
#define RANGE_STATUS            0x04d
// Interrupt status
#define INTERRUPT_STATUS        0x04f
// Range reading value
#define RANGE_VAL               0x062

/ Class for managing connection and state to a VL6180X sensor
class Adafruit_VL6180X {
 public:
  Adafruit_VL6180X();
  uint8_t Read(void);
  uint8_t readRangeStatus(void);

 private:
  void loadSettings(void);
    \\write values to the bit
  void write8(uint16_t address, uint8_t data);
  void write16(uint16_t address, uint16_t data);
    \\read values from the register
  uint16_t read16(uint16_t address);
  uint8_t read8(uint16_t address);
};
```

LISTING A.1: Arduino VL6180x -Header

```
int VL6180X_Init() {
char reset;
reset = ReadByte(SYSTEM_RESET);
if (reset==1){                    %check initialization
load_settings();                  %load initial settings
WriteByte(SYSTEM_RESET, 0x00);    %change status to 0
}
return 0;
}
```

LISTING A.2: Arduino VL6180x - Initialization

A.2 DRV2605 Motor Driver

```
#include <Wire.h>
#define DRV2605_ADDR 0x5A             // Device I2C address

#define STATUS              0x00       // Status register
#define MODE                0x01         // Mode register
#define MODE_PWMANALOG      0x03   // PWM/Analog input mode
#define MODE_AUTOCAL        0x078   // Auto cal mode
#define RATEDV          0x16       // Rated voltage register
#define CLAMPV          0x17       // Overdrive clamp voltage
#define CALCOMP         0x18  // Auto-cal compensation register
#define CALEMP          0x19   // Auto-cal back-EMF register
#define FEEDBACK        0x1A     // Feedback control register
#define CONTROL1        0x1B     // Control1 Register
#define CONTROL2        0x1C     // Control2 Register
#define CONTROL3        0x1D     // Control3 Register
#define CONTROL4        0x1E     // Control4 Register

\\function declaration
class Adafruit_DRV2605 {
  public:
    Adafruit_DRV2605(void);
    boolean init();
    void writeRegister8(uint8_t reg, uint8_t val);
    uint8_t readRegister8(uint8_t reg);
    void setMode(uint8_t mode);
    void useERM();
    void useLRA();

  private:
    TwoWire *_wire;
};

\begin{lstlisting}[label={list:tenth}, caption=DRV2605 -
   Initialization for LRA]
void motor_init() {
_wire->begin();
writeRegister8(MODE, 0x00);  %Remove from standby
writeRegister8(OVERDRIVE, 0x00);  % no overdrive
writeRegister8(FEEDBACK, 0xB6); %LRA mode
writeRegister8(CONTROL1, 0x17); %Set LRA drive time
writeRegister8(CONTROL2, 0xF5); %Set LRA sampling time = 300 s
writeRegister8(CONTROL3, 0x80); %Set LRA PWM-input mode
}
```

LISTING A.3: DRV2605 - Header

Appendix B

Mechanical Design

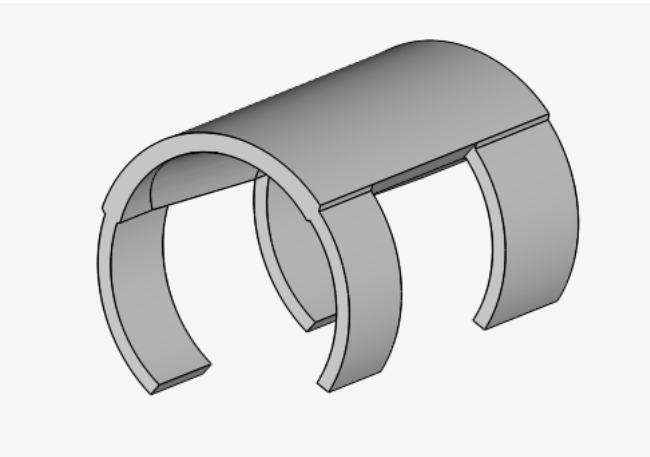

FIGURE B.1: Prototype 1: First prototype to test the fit on the finger based on the optimal width

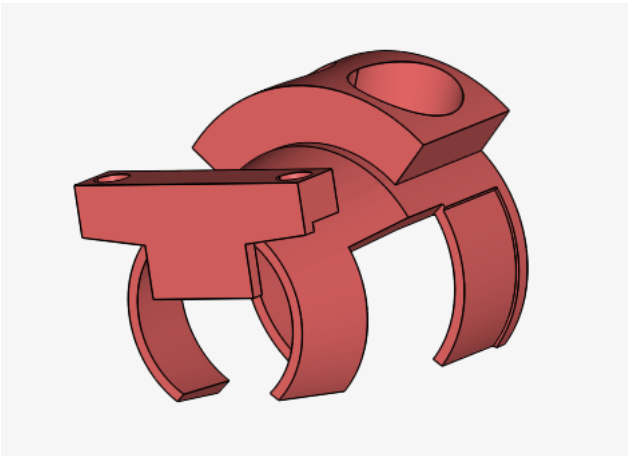

FIGURE B.2: Prototype 2: Initial prototype to test position of the actuators on the upper side of the body. Even with some dampers placed between the actuators and the main body, the vibrations spread through most of the structure.

Appendix C

Questionnaire